bioRxiv preprint doi: https://doi.org/10.1101/132696; this version posted June 8, 2017. The copyright holder for this preprint (which was not certified by peer review) is the author/funder. All rights reserved. No reuse allowed without permission.

Title: A high resolution atlas of gene expression in the domestic sheep (*Ovis aries*)

Clark EL[1ø*], Bush SJ[1ø], McCulloch MEB[1], Farquhar IL[1‡], Young R[1], Lefevre L[1], Pridans C[1], Tsang HG[1], Wu C[2], Afrasiabi C[2], Watson M[1], Whitelaw CB[1], Freeman TC[1], Summers KM[1], Archibald AL[1] and Hume DA[1]

[1]The Roslin Institute and Royal (Dick) School of Veterinary Studies, University of Edinburgh, Easter Bush Campus, Edinburgh, Midlothian, EH25 9RG.

[2]Department of Integrative and Computational Biology, The Scripps Research Institute, 10550 North Torrey Pines Road, La Jolla, CA 92037.

[‡]Current Address: Centre for Synthetic and Systems Biology, CH Waddington Building, Max Borne Crescent, Kings Buildings, University of Edinburgh, EH9 3BF.

[ø] These two authors contributed equally to the work.

* Corresponding Author: emily.clark@roslin.ed.ac.uk

bioRxiv preprint doi: https://doi.org/10.1101/132696; this version posted June 8, 2017. The copyright holder for this preprint (which was not certified by peer review) is the author/funder. All rights reserved. No reuse allowed without permission.

Abstract

Sheep are a key source of meat, milk and fibre for the global livestock sector, and an important biomedical model. Global analysis of gene expression across multiple tissues has aided genome annotation and supported functional annotation of mammalian genes. We present a large-scale RNA-Seq dataset representing all the major organ systems from adult sheep and from several juvenile, neonatal and prenatal developmental time points. The *Ovis aries* reference genome (Oar v3.1) includes 27,504 genes (20,921 protein coding), of which 25,350 (19,921 protein coding) had detectable expression in at least one tissue in the sheep gene expression atlas dataset. Network-based cluster analysis of this dataset grouped genes according to their expression pattern. The principle of 'guilt by association' was used to infer the function of uncharacterised genes from their co-expression with genes of known function. We describe the overall transcriptional signatures present in the sheep gene expression atlas and assign those signatures, where possible, to specific cell populations or pathways. The findings are related to innate immunity by focusing on clusters with an immune signature, and to the advantages of cross-breeding by examining the patterns of genes exhibiting the greatest expression differences between purebred and crossbred animals. This high-resolution gene expression atlas for sheep is, to our knowledge, the largest transcriptomic dataset from any livestock species to date. It provides a resource to improve the annotation of the current reference genome for sheep, presenting a model transcriptome for ruminants and insight into gene, cell and tissue function at multiple developmental stages.

bioRxiv preprint doi: https://doi.org/10.1101/132696; this version posted June 8, 2017. The copyright holder for this preprint (which was not certified by peer review) is the author/funder. All rights reserved. No reuse allowed without permission.

Author Summary

Sheep are ruminant mammals kept as livestock for the production of meat, milk and wool in agricultural industries across the globe. Genetic and genomic information can be used to improve production traits such as disease resiliance. The sheep genome is however missing important information relating to gene function and many genes, which may be important for productivity, have no informative gene name. This can be remedied using RNA-Sequencing to generate a global expression profile of all protein-coding genes, across multiple organ systems and developmental stages. Clustering genes based on their expression profile across tissues and cells allows us to assign function to those genes. If for example a gene with no informative gene name is expressed in macrophages and is found within a cluster of known macrophage related genes it is likely to be involved in macrophage function and play a role in innate immunity. This information improves the quality of the reference genome and provides insight into biological processes underlying the complex traits that influence the productivity of sheep and other livestock species.

Introduction

Sheep (*Ovis aries*) represent an important livestock species globally and are a key source of animal products including meat, milk and fibre. They remain an essential part of the rural economy in many developed countries and are central to sustainable agriculture in developing countries. They are also an important source of greenhouse gases [1]. Although genetic improvement is often considered to have been less effective in sheep than in the dairy cattle, pig and poultry sectors, advanced genomics-enabled breeding schemes are being implemented in New Zealand and elsewhere [2-4]. A better understanding of functional sequences, including transcribed sequences and the transcriptional control of complex traits

bioRxiv preprint doi: https://doi.org/10.1101/132696; this version posted June 8, 2017. The copyright holder for this preprint (which was not certified by peer review) is the author/funder. All rights reserved. No reuse allowed without permission.

such as disease resilience, reproductive capacity, feed conversion efficiency and welfare, will enable further improvements in productivity with concomitant reductions in environmental impact.

RNA-Sequencing (RNA-Seq) has transformed the analysis of gene expression from the single-gene to the genome-wide scale allowing visualisation of the transcriptome and re-defining how we view the transcriptional control of complex traits (reviewed in [5]). Large-scale gene expression atlas projects have defined the mammalian transcriptome in multiple species, initially using microarrays [6-9] and more recently by the sequencing of full length transcripts or of 5' ends, for example in the horse [10], and in human and mouse by the FANTOM 5 consortium [11-13], ENCODE project [14] and Genotype-Tissue Expression (GTEx) Consortium [15].

These efforts have focused mainly on mice and humans, for which there are high quality richly annotated reference genome sequences available as a frame of reference for the identification and analysis of transcribed sequences. Draft reference genome sequences have been established for the major livestock species (chicken, pig, sheep, goat and cattle) over the past decade, yet it is only with the recent deployment of long read sequencing technology that the contiguity of the reference genome sequences for these species has improved. This is exemplified by the recent goat genome assembly [16, 17]. In these species there are still many predicted protein-coding and non-coding genes for which the gene model is incorrect or incomplete, or where there is no informative functional annotation. For example, in the current sheep reference genome, Oar v3.1 (Ensembl release 87) (http://www.ensembl.org/Ovis_aries/Info/Index), 30% of protein-coding genes are identified with an Ensembl placeholder ID [18]. Given the high proportion of such unannotated genes many are likely to be involved in important functions. Large-scale RNA-Seq gene expression datasets can be utilised to understand the underlying biology and annotate and

bioRxiv preprint doi: https://doi.org/10.1101/132696; this version posted June 8, 2017. The copyright holder for this preprint (which was not certified by peer review) is the author/funder. All rights reserved. No reuse allowed without permission.

assign function to such unannotated genes [19]. With sufficiently large datasets, genes form co-expression clusters, which can either be generic, associated with a given pathway or be cell-/tissue- specific. This information can then be used to associate a function with genes co-expressed in the same cluster, a logic known as the 'guilt by association principle' [20]. Detailed knowledge of the expression pattern can provide a valuable window on likely gene function, as demonstrated in pig [6], sheep [18, 21], human and mouse [8, 9, 22, 23].

A high quality well-annotated reference genome is an exceptionally valuable resource for any livestock species, providing a comparative sequence dataset and a representative set of gene models. The International Sheep Genomics Consortium (ISGC) released a high quality draft sheep genome sequence (Oar v3.1) in 2014 [18]. Included in the sheep genome paper were 83 RNA-Seq libraries from a Texel gestating adult female, 16 day embryo, 8 month old lamb and an adult ram. This Texel RNA-Seq transcriptome significantly improved the annotation of Oar v3.1 and identified numerous genes exhibiting changes in copy number and tissue specific expression [18]. To build on this resource and further improve the functional annotation of Oar v3.1 we have generated a much larger high-resolution transcriptional atlas from a comprehensive set of tissues and cell types from multiple individuals of an outbred cross of two economically important sheep breeds. To maximize heterozygosity we deliberately chose a cross of disparate breeds, the Texel, which is used as a terminal sire as it is highly muscled in some cases because it has a myostatin variant linked to double-muscling and meat quality [24], and the Scottish Blackface, a breed selected for robustness on marginal upland grazing [25].

The sheep gene expression atlas dataset presented here is the largest of its kind from any livestock species to date and includes RNA-Seq libraries from tissues and cells representing all the major organ systems from adult sheep and from several juvenile, neonatal and prenatal developmental time points. Because the tissues were obtained from multiple

bioRxiv preprint doi: https://doi.org/10.1101/132696; this version posted June 8, 2017. The copyright holder for this preprint (which was not certified by peer review) is the author/funder. All rights reserved. No reuse allowed without permission.

126 healthy young adult animals, the atlas may also aid understanding of the function of
127 orthologous human genes. Our aim was to provide a model transcriptome for ruminants and
128 give insight into gene, cell and tissue function and the molecular basis of complex traits. To
129 illustrate the value of the resource, we provide detailed examination of genes implicated in
130 innate immunity and the advantages of cross breeding and provide putative gene names for
131 hundreds of the unannotated genes in Oar v3.1. The entire data set is available in a number of
132 formats to support the research community and will contribute to the Functional Annotation
133 of Animal Genomes (FAANG) project [26, 27].
134

135 ## Results and Discussion

136 ### Scope of Sheep Gene Expression Atlas Dataset

137 This sheep gene expression atlas dataset expands on the RNA-Seq datasets already
138 available for sheep, merging a new set of 429 RNA-Seq libraries from the Scottish Blackface
139 x Texel cross (BFxT) with 83 existing libraries from Texel [18]. Details of the new BFxT
140 libraries generated for the sheep gene expression atlas, including the developmental stages
141 sampled, tissue/cell types and sex of the animals are summarised in Table 1. These samples
142 can be grouped into 4 subsets ("Core Atlas", "GI Tract Time Series", "Early Development"
143 and "Maternal Reproductive Time Series"). The animals used to generate the four subsets of
144 samples are detailed in S1 Table.
145

146 **Table 1: Details of the tissues and cell types sequenced to generate the BFxT RNA-Seq**
147 **dataset for the sheep gene expression atlas.**
148

Subset	Tissue Type	Library Type	Sequencing Depth	Total Number of Libraries	Number of Individuals
Core Atlas	Liver, spleen, ovary, testes,	Total RNA-Seq	>100 million reads per	60 (10 per individual)	3 adult males and 3 adult

bioRxiv preprint doi: https://doi.org/10.1101/132696; this version posted June 8, 2017. The copyright holder for this preprint (which was not certified by peer review) is the author/funder. All rights reserved. No reuse allowed without permission.

	hippocampus, kidney medulla, bicep muscle, reticulum, ileum, thymus, left ventricle		sample		females
Core Atlas	GI tract, reproductive tract, brain, endocrine, cardiovascular, lymphatic, musculo-skeletal, immune cells	mRNA-Seq	>25 million reads per sample	248 (~45 per individual)	3 adult males and 3 adult females
LPS Time Course (Core Atlas)	BMDM 0h (-LPS) and 7h (+LPS)	Total RNA-Seq	>100 million reads per sample	12 (2 time points per individual)	3 adult males and 3 adult females
LPS Time Course (Core Atlas)	BMDM 2h, 4h, 24h post LPS treatment	mRNA-Seq	>25 million reads per sample	32 (3 time points per individual)	3 adult males and 3 adult females
GI Tract Time Series	Gastro-intestinal tract	mRNA-Seq	>25 million reads per sample	90 (10 tissues per individual)	9 lambs (3 at birth, 3 at one week and 3 at 8 weeks)
Early Development (blastocysts)	Day 7 blastocysts (3 pools of 8)	Nu Gen Single Cell Ovation Kit	>66 million reads per sample	3	3 pools
Early Development (day 23)	Day 23 whole embryos	Total RNA-Seq	>100 million reads per sample	3	3
Early Development (day 35)	Liver, brain, embryonic fibroblasts	mRNA-Seq	>25 million reads per sample	7	3 embryos (two female and one male)
Early Development (day 100)	Liver, ovary	mRNA-Seq	>25 million reads per sample	5	3 female (liver) 2 female (ovary)
Maternal Reproductive Time Series (days, 23, 35 and 100)	Placenta and ovary	mRNA-Seq	>25 million reads per sample	12	2 females per time point

Tissues and cells were chosen to cover all major organ systems. All libraries were Illumina 125bp paired end stranded libraries. See S2 Table for a detailed list of the tissues and cell types sequenced.

The "Core Atlas" subset was generated using six adult virgin sheep, approximately 2 years of age. Tissue samples were collected from all major organ systems from 3 males and 3 females to ensure, wherever possible, there were biological replicates from each sex to

bioRxiv preprint doi: https://doi.org/10.1101/132696; this version posted June 8, 2017. The copyright holder for this preprint (which was not certified by peer review) is the author/funder. All rights reserved. No reuse allowed without permission.

support an analysis of sex-specific gene expression. In addition, five cell types were sampled, including peripheral blood mononuclear cells (PBMCs) and blood leukocytes. Since macrophages are known to be a highly complex source of novel mRNAs [28], and were not sampled previously, three types of macrophage (+/- stimulation with lipopolysaccharide (LPS)) were included.

For the "GI Tract Time Series" subset of samples we focused on 10 regions of the gastro-intestinal (GI) tract, immediately at birth prior to first feed, at one week and at 8 weeks of age. These time points aimed to capture the transition from milk-feeding to rumination. Embryonic time points were chosen, at days 23, 35 and 100, to detect transcription in the liver, ovary and brain in "Early Development". Parallel time points were included for placenta and ovary samples from gestating BFxT ewes, comprising the "Maternal Reproductive Time Series" subset. Finally, 3 pools of eight day 7 blastocysts were included to measure transcription pre-implantation and these were also included in the "Early Development" subset.

A detailed list of all tissues and cell types included in each subset of samples can be found in S2 Table. Tissues and cell types were chosen to give as comprehensive a set of organ systems as possible and include those tissues relevant for phenotypic traits such as muscle growth and innate immunity.

Sequencing Depth and Coverage

Approximately $37x10^9$ sequenced reads were generated from the BFxT libraries, generating approximately $26x10^9$ alignments in total. The raw number of reads and percentage of alignable reads per sample are included in S3 Table. For each tissue a set of expression estimates, as transcripts per million (TPM), were obtained using the high speed transcript quantification tool Kallisto [29]. Kallisto is a new transcriptome-based

bioRxiv preprint doi: https://doi.org/10.1101/132696; this version posted June 8, 2017. The copyright holder for this preprint (which was not certified by peer review) is the author/funder. All rights reserved. No reuse allowed without permission.

quantification tool that avoids the considerable bias introduced by the genome alignment step [30]. Gene level expression atlases are available as S1 Dataset and, with expression estimates averaged per tissue per developmental stage, S2 Dataset. The data were corrected for library type (as we described in [31] and summarised in S1 Methods). We used Principal Component Analysis (PCA) pre- and post-correction (S1 Fig) for library type to ensure the correction was satisfactory. Hierarchical clustering of the samples is included in (Fig 1) and illustrates both the large diversity and logical clustering of samples of samples included in the dataset.

The *O. aries* reference genome (Oar v3.1) includes 27,504 loci that are transcribed (20,921 protein coding), of which 25,350 (19,921 protein coding) (97%) were detectable with expression of TPM >1, in at least one tissue from at least one individual, in the sheep gene expression atlas dataset, demonstrating the depth and scope of this dataset. The proportion of transcripts with detectable expression, after each 'pass' with Kallisto (See Materials and Methods), is presented in Table 2. Only 3% (561) of transcripts from Oar v3.1 (S4 Table) did not meet the minimum detection threshold of TPM > 1 in at least one tissue and therefore were not detected in the sheep atlas dataset. In a minority of cases, transcripts were missing because they were highly specific to a tissue or cell which was not sampled, such as odontoblasts (which uniquely produce tooth dentin, mediated by DSPP (dentin sialophosphoprotein) [32]). We also did not include any samples taken from the eye which expresses multiple unique proteins e.g., the lens-specific enzyme LGSN (lengsin) [33]. The majority (77%) of the genes not detected in the sheep atlas were unannotated, with no assigned gene name. A small number of these genes (36) lack sequence conservation and coding potential and so are potentially spurious models (S4 Table).

Table 2: The number and percentage of Oar v3.1 protein coding and non-coding genes, with average TPM across all animals > 1 in at least one tissue, in both the BFxT dataset

bioRxiv preprint doi: https://doi.org/10.1101/132696; this version posted June 8, 2017. The copyright holder for this preprint (which was not certified by peer review) is the author/funder. All rights reserved. No reuse allowed without permission.

after the Kallisto first and second pass, and after incorporating the existing Texel dataset.

RNA-Seq data used:	**Scottish Blackface x Texel Libraries Only**					**Including the existing Texel dataset**	
Kallisto index:	First-Pass			Second-Pass (restricted)		Second-Pass (restricted)	
Gene type	No. in reference annotation (Oar v3.1)	No. of genes of this type expressed	% genes of this type expressed	No. of genes of this type expressed	% genes of this type expressed	No. of genes of this type expressed	% genes of this type expressed
lincRNA	1858	1548	83.32	0	0	0	0
miRNA	1305	1242	95.17	0	0	0	0
misc RNA	361	310	85.87	0	0	0	0
MT rRNA	2	2	100	0	0	0	0
MT tRNA	22	19	86.36	0	0	0	0
processed pseudogene	43	31	72.09	35	81.40	38	88.37
protein-coding	20921	19921	95.22	20189	96.50	20359	97.31
pseudogene	247	172	69.64	189	76.52	201	81.38
rRNA	305	272	89.18	0	0	0	0
snoRNA	756	717	94.84	0	0	0	0
snRNA	1234	1116	90.44	0	0	0	0
Sum	**27054**	**25350**		**20413**		**20598**	

'BFxT data' refers to the present study; 'Texel data' is obtained from [18]. The 'first pass' Kallisto index contains the known *Ovis aries* v3.1 cDNAs for both protein-coding and non-protein coding transcripts. The 'second pass' Kallisto index is a filtered version of the former, that (a) restricts the RNA space to protein-coding genes, pseudogenes, and processed pseudogenes (so that expression within an equivalent space will be quantified, irrespective of experimental protocol), (b) omits genes that had no detectable expression across all BFxT

bioRxiv preprint doi: https://doi.org/10.1101/132696; this version posted June 8, 2017. The copyright holder for this preprint (which was not certified by peer review) is the author/funder. All rights reserved. No reuse allowed without permission.

215 samples, and (c) includes novel transcript reconstructions further to the *de novo* assembly of
216 unmapped reads.
217
218 **Gene Annotation**
219 In the Oar v3.1 annotation, 6217 (~30%) of the protein coding genes lack an
220 informative gene name. Whilst the Ensembl annotation will often identify homologues of a
221 sheep gene model, the automated annotation pipeline used is conservative in its assignment
222 of gene names and symbols. Using an annotation pipeline (described in S1 Methods and
223 illustrated in S5 Table) we were able to utilise the sheep gene expression atlas dataset to
224 annotate >1000 of the previously unannotated protein coding genes in Oar v3.1 (S6 Table).
225 These genes were annotated by reference to the NCBI non-redundant (nr) peptide database
226 v77 [34] and assigned a quality category based on reciprocal percentage identity, if any, to
227 one of 9 known ruminant proteomes (S7 Table). A short-list containing a conservative set of
228 gene annotations, to HGNC (HUGO Gene Nomenclature Committee) gene symbols, is
229 included in S8 Table. Many of these genes are found in syntenic regions, and are
230 also supported by the up- and downstream conservation of genes in a related genome, cattle
231 (*Bos taurus* annotation UMD 3.1). S9 Table contains the full list of genes annotated using
232 this pipeline. Many unannotated genes can be associated with a gene description, but not
233 necessarily an HGNC symbol; these are also listed in S10 Table. We manually validated the
234 assigned gene names on this longer list using network cluster analysis and the "guilt by
235 association" principle.
236
237 **Network Cluster Analysis**
238 Network cluster analysis of the sheep gene expression atlas was performed using
239 Miru (Kajeka Ltd, Edinburgh UK), a tool for the visualisation and analysis of network graphs

bioRxiv preprint doi: https://doi.org/10.1101/132696; this version posted June 8, 2017. The copyright holder for this preprint (which was not certified by peer review) is the author/funder. All rights reserved. No reuse allowed without permission.

from big data [35-37]. The the atlas of unaveraged TPM estimates, available as S1 Dataset, were used for the network cluster analysis. The three blastocyst samples were removed from the network cluster analysis as they were generated using a library preparation method which was not corrected for and created a significant effect of library type. With a Pearson correlation co-efficient threshold of r=0.75 and MCL (Markov Cluster Algorithm [38]) inflation value of 2.2, the gene-to-gene network comprised 15,129 nodes (transcripts) and 811,213 edges (correlations above the threshold value). This clustering excludes >30% of detected transcripts, most of which had idiosyncratic expression profiles. One of the major sources of unique expression patterns is the use of distinct promoters in different cell types. The transcription factor *MITF* (Melanogenesis Associated Transcription Factor), for example, does not cluster with any other transcripts in sheep and is known in humans to have at least 7 distinct tissue-specific promoters in different cell types, including macrophages, melanocytes, kidney, heart and retinal pigment epithelium [13].

The resultant correlation network (Fig 2) was very large and highly structured comprising of 309 clusters ranging in size. Genes found in each cluster are listed in S11 Table and clusters 1 to 50 (numbered in order of size; cluster 1 being made up of 1199 genes) were annotated by hand and assigned a broad functional 'class' and 'sub-class' (Table 3). Functional classes were assigned based on GO term enrichment [39] for molecular function and biological process (S12 Table) and gene expression pattern, as well as comparison with functional groupings observed in the pig expression atlas [6]. Fig 3 shows a network graph with the nodes collapsed, and the largest clusters numbered 1 to 30, to illustrate the relative number of genes in each cluster and their functional class.

Table 3: Tissue/cell/pathway association of the largest 50 network clusters in the sheep gene expression atlas dataset.

bioRxiv preprint doi: https://doi.org/10.1101/132696; this version posted June 8, 2017. The copyright holder for this preprint (which was not certified by peer review) is the author/funder. All rights reserved. No reuse allowed without permission.

Cluster ID	Number of Transcripts	Profile Description	Class	Sub-Class
1	1199	General	House Keeping	House Keeping (1)
2	987	Brain	CNS	CNS
3	658	Testes – Adult	Reproduction	Gamete Production
4	585	General	House Keeping	House Keeping (2)
5	351	Macrophages	Immune	Macrophages
6	350	Fallopian Tube > Testes	Cilia	Motile Cilia
7	284	Fetal Ovary > Adult Testes	Early Development	Reproduction
8	276	Many Tissues - Highly Variable	Pathway	Cell Cycle
9	265	Fetal Brain > Adult Brain	CNS	CNS
10	247	Skeletal Muscle > Oesophageal Muscle	Musculature	Skeletal Muscle
11	219	Lymph Nodes > Blood > Not Macrophages	Immune	T-Cell and B-Cell
12	215	Thymus > Salivary Gland	Immune	T-Cell
13	186	Fore-Stomachs > Tonsil > Skin	GI Tract	Ruminal Epithelium
14	183	Kidney Cortex > Liver	Renal	Kidney Cortex
15	182	General but not even - highest in muscle	Pathway	Oxidative Phosphorylation
16	158	Epididymis > Vas Deferens	Reproduction	Male
17	153	Liver	Liver	Liver (Hepatocytes)
18	145	Peyer's Patch, Ileum, Lymph Nodes, Blood	Immune	T-Cell and B-Cell
19	134	Placenta	Gestation	Placental Function
20	119	Epididymis > Testes > Vas Deferens	Reproduction	Male
21	115	General but not even	Pathway	Ribosomal
22	102	Adrenal Gland	Endocrine	Steroid Hormone Biosynthesis
23	102	Placenta	Gestation	Placental Function
24	98	Liver > Small Intestine	Liver	Liver (GI Tract)
25	96	Fetal Liver	Liver	Developing Liver
26	92	Small Intestine > Large Intestine	GI tract	GI Tract
27	90	Pituitary Gland	Endocrine	Hormone Synthesis
28	85	General highest in reproductive tissues and brain	Cilia	Primary Cilia
29	77	Heart	Musculature	Cardiac Muscle
30	75	Thyroid	Endocrine	Thyroxine Synthesis
31	73	Peyers Patch, Ileum, Lymph Nodes, Blood, Macrophages	Immune	T-Cell and B-Cell
32	69	Salivary Gland, Lymph Node, Blood, Small Intestine	Immune	T-Cell and B-Cell
33	68	Fore-Stomachs Adult - Not Neonates > AMs	GI Tract	Immune
34	65	Small Intestine > Large Intestine	GI tract	GI Tract
35	61	General - highest in brain	House Keeping	House Keeping (3)

bioRxiv preprint doi: https://doi.org/10.1101/132696; this version posted June 8, 2017. The copyright holder for this preprint (which was not certified by peer review) is the author/funder. All rights reserved. No reuse allowed without permission.

36	58	Heart Valves	Cardiovascular	Extra Cellular Matrix
37	58	General - highest in blood	House Keeping	House Keeping (4)
38	56	General - highest in fetal brain	House Keeping	House Keeping (5)
39	50	GI Tract - highest in reticulum	GI Tract	GI Tract
40	49	General - highest in testes	House Keeping	House Keeping (6)
41	49	General - highest in ovary	House Keeping	House Keeping (7)
42	47	General - highest in brain	House Keeping	House Keeping (8)
43	45	Fore-Stomachs > Tonsil > Skin	GI Tract	Ruminal Epithelium
44	45	General - highest in testes	House Keeping	House Keeping (9)
45	44	Macrophage (BMDM + LPS)	Immune	Macrophages (LPS Response TNF)
46	44	Blood, Lymph Nodes	Immune	Blood
47	42	Large Intestine	GI Tract	GI Tract
48	42	General	Pathway	Histones
49	41	Reticulum and Rumen - very variable	GI Tract	Reticulum/Rumen
50	36	Adrenal Gland Medulla	Endocrine	Steroid Hormone Biosynthesis

The majority of co-expression clusters included genes exhibiting a specific cell/tissue expression pattern (Fig 4A). There were a few exceptions, including the largest cluster (cluster 1), which contained ubiquitously expressed 'house-keeping' genes, encoding proteins that are functional in all cell types. The high proportion of unannotated genes (24% of the 1199 genes) in cluster 1 may reflect the focus of functional genomics on genes exhibiting tissue specific expression, and inferred function in differentiation, leaving those with a house-keeping function uncharacterised [40]. With a few exceptions, the remaining co-expression clusters were comprised of genes exhibiting either expression only in a distinct tissue or cell type expression pattern e.g. macrophages (cluster 5) (Fig 4B (i)) and fetal ovary (cluster 7) (Fig 4B (ii)), or a broader expression pattern associated with a cellular process e.g. oxidative phosphorylation (cluster 15) (Fig 4B (iii)). Some co-expression is shared between two or more organ systems, associated with known shared functions. For example, cluster 15, exhibiting high expression in liver and kidney cortex, is enriched for expression of genes relating to the oxidation-reduction process, transmembrane transport, monocarboxylic acid

bioRxiv preprint doi: https://doi.org/10.1101/132696; this version posted June 8, 2017. The copyright holder for this preprint (which was not certified by peer review) is the author/funder. All rights reserved. No reuse allowed without permission.

catabolic process and fatty acid oxidation (S13 Table). It includes numerous genes encoding enzymes involved in amino acid catabolism (e.g. *AGXT*, *AGXT2*, *ASPDH*, *ACY1*, *EHHADH*, *DPYD*, *DAO*, *DDO*, *HAO1*, and *HPD*) and the rate-limiting enzymes of gluconeogenesis (*PCK1*, *PC*, *ALDOB* and *G6PC*). The contributions of kidney and liver to amino acid turnover and gluconeogenesis are well known in humans [41] and rodents [42]. These observations suggest that the shared catabolic pathways of liver and kidney cortex are largely conserved in sheep, but detailed curation of the genes in this cluster could provide further specific insights. Alanine aminotransferase (*ALT1* synonym *GPT1*), which generates alanine from the breakdown of amino acids in muscle and is transported to the liver for gluconeogenesis, is highly-expressed in muscle as expected. The glutaminase genes, required for the turnover of glutamine, are absent from tissue or cell type specific clusters; the liver-specific enzyme *GLS2* is also expressed in neuronal tissues, as it is in humans [43, 44].

The tissue-specific expression patterns observed across clusters showed a high degree of similarity to those observed for pig [6], human and mouse [8, 9]. In some cases we were able to add functional detail to clusters of genes previously observed in pig and human. For example, genes within cluster 6 showed high expression in the fallopian tube and to a lesser extent the testes. Significantly enriched GO terms for cluster 6 included cilium ($p=4.1x10^{-8}$), microtubule motor activity ($p=2.9x10^{-11}$) and motile cilium ($p=2.8x10^{-19}$) suggesting the genes expressed in cluster 6 are likely to have a function related to motile cilia in sperm cells and the fallopian tube. Cluster 6 in the sheep atlas dataset corresponds to cluster 9 in the pig gene expression atlas [6]. Similarly, significantly enriched GO terms for genes in cluster 28 included primary cilium ($p=7.5x10^{-21}$) and ciliary basal body ($p=1.9x10^{-12}$), indicating the genes in this cluster were associated with the function of primary cilia. Genes within this cluster showed a relatively wide expression pattern, with brain and reproductive tissues

bioRxiv preprint doi: https://doi.org/10.1101/132696; this version posted June 8, 2017. The copyright holder for this preprint (which was not certified by peer review) is the author/funder. All rights reserved. No reuse allowed without permission.

exhibiting the highest expression. For both clusters associated with cilial function, significantly enriched GO terms also included cell-cycle related cellular processes and cell-cycle associated genes, supporting the link between cilia and the cell-cycle [45-47].

Cellular Processes

The genes within some clusters, rather than being linked to the function of a particular tissue or cell type, showed varying levels of expression across multiple tissues, suggesting their involvement in a universal cellular process (pathway). Significantly enriched GO terms for genes in cluster 8, for example, included 'cell cycle checkpoint' ($p=1x10^{-17}$) and 'mitotic cell cycle' ($p=<1x10^{-30}$). The variation in expression of these genes across tissues likely reflects variation in the proportion of mitotically active cells. In the same way, it is possible to extract a similar cluster from large cancer gene expression data sets, correlating with their proliferative index [48]. Expression of genes in cluster 15 (n=182) was detectable in most ovine tissues and cells but with strongly-enriched expression in skeletal and cardiac muscle. The pig gene expression atlas [6] highlighted an oxidative phosphorylation cluster and a mitochondrial/tricarboxylic acid (TCA) cluster. This functional grouping is merged in cluster 15. The majority of the transcripts in cluster 15 are present within the inventory of mitochondrial genes in humans and mice [49], but the reciprocal is not true since many other genes encoding proteins that locate to mitochondria were not found in cluster 15. Many mitochondrial proteins are unrelated to oxidative phosphorylation *per se*, and are enriched in other tissues including liver and kidney (including mitochondrial enzymes of amino acid and fatty acid catabolism, see above) and intestine.

Cluster 15 also contains several genes associated with myosin and the sarcoplasmic reticulum which may indicate some level of coordination of their function with the oxidative metabolism of glucose. The majority of genes in the corresponding cluster in pig [6] were

bioRxiv preprint doi: https://doi.org/10.1101/132696; this version posted June 8, 2017. The copyright holder for this preprint (which was not certified by peer review) is the author/funder. All rights reserved. No reuse allowed without permission.

also present in this cluster with a few notable additions including dihydrolipoamide dehydrogenase (*DLD*), which encodes a member of the class-I pyridine nucleotide-disulfide oxidoreductase family, and carnitine acetyltransferase (*CRAT*), a key enzyme in the metabolic pathway in mitochondria [50]. We were able to assign gene names to the following genes associated with oxidative phosphorylation complex I in pig: *NDUFA9* (ENSOARG00000009435), *NDUFB1* (ENSOARG00000020197), *NUDFB8* (assigned to ENSOARG00000015378), and *NDUFC2* (ENSOARG00000006694). The gene name *PTGES2* (prostaglandin E2 synthase 2) was assigned to ENSOARG00000010878, a gene that was associated with fatty acid (long-chain) beta oxidation in pig [6] but previously unannotated in sheep. Similarly, we assigned the gene name *PDHB* (pyruvate dehydrogenase E1 component subunit beta), a member of the pyruvate dehydrogenase complex also previously unannotated in sheep, to ENSOARG00000012222. The inclusion of the PDH complex, as well as the mitochondrial pyruvate carriers *MPC1* and *MPC2*, in the muscle-enriched cluster 15 reflects the fact that glucose, giving rise to pyruvate, is the preferred fuel for oxidative metabolism in muscle [51].

By using comparative clustering information in the pig and the "guilt by association" principle we were able to assign with confidence gene names and putative function to the majority of unannotated genes in clusters 8 (cell-cycle) and 15 (oxidative phosphorylation) (S13 Table). Expression of cell cycle and metabolic genes has recently been shown to be positively correlated with dry matter intake, ruminal short chain fatty acid concentrations and methane production in sheep [52]. In the same study a weak correlation between lipid/oxo-acid metabolism genes and methane yield was also identified suggesting that the newly unannotated genes in these clusters are likely to be relevant in addressing methane production in ruminants [52].

bioRxiv preprint doi: https://doi.org/10.1101/132696; this version posted June 8, 2017. The copyright holder for this preprint (which was not certified by peer review) is the author/funder. All rights reserved. No reuse allowed without permission.

355 **The GI Tract**

356 Stringent coexpression clustering requires that each transcript is quantified in a
357 sufficiently large number of different states to establish a strong correlation with all other
358 transcripts with which it shares coordinated transcription and, by implication, a shared
359 function or pathway. The impact of this approach was evident from the pig gene expression
360 atlas [6] which was effective at dissecting region-specific gene expression in the GI tract. We
361 have generated a comparable dataset for sheep. In ruminants, the rumen, reticulum and
362 omasum are covered exclusively with stratified squamous epithelium similar to that observed
363 in the tonsil [18, 21]. Each of these organs has a very distinctive mucosal structure, which
364 varies according to region sampled [53]. A network cluster analysis of regions of the GI tract
365 from sheep has been published [21] using the Texel RNA-Seq dataset [18]. These co-
366 expression clusters are broken up somewhat in this larger atlas, because many of the genes
367 that are region-specific in the GI tract are also expressed elsewhere. We have, in addition,
368 expanded the available dataset for the GI tract to include samples from neonatal and juvenile
369 lambs.

370 The postnatal development of the sheep GI tract is of particular interest because of the
371 pre-ruminant to ruminant transition, which occurs over 8 weeks from birth. Genes in cluster
372 33 showed low levels of expression in neonatal lambs and a gradual increase into adulthood.
373 Enriched GO terms for this cluster include regulation of interleukin 6 (IL6) production
374 ($p=0.0016$) and keratinocyte differentiation ($p=1.7x10^{-8}$) (S12 Table). The cluster includes
375 genes such as *HMGCS2*, *HMGCL* and *BDH1*, required for ketogenesis, an essential function
376 of rumen metabolism, as well as *CA1* (carbonic anhydrase 1), implicated in the rumen-
377 specific uptake of short chain fatty acids. The cluster does not contain any of the solute
378 carriers implicated in nutrient uptake in the rumen, suggesting that these are more widely-
379 expressed and/or regulated from multiple promoters [21]. The only carrier that is rumen-

bioRxiv preprint doi: https://doi.org/10.1101/132696; this version posted June 8, 2017. The copyright holder for this preprint (which was not certified by peer review) is the author/funder. All rights reserved. No reuse allowed without permission.

enriched is *SLC9A3* (also known as *NHE3*), the key Na-H antiporter previously implicated in rumen sodium transport in both sheep and cattle [54]. Other genes in cluster 33, for example, *IL36A* and *IL36B*, for example, are thought to influence skin inflammatory response by acting on keratinocytes and macrophages and indirectly on T-lymphocytes to drive tissue infiltration, cell maturation and cell proliferation [55]. Many of these genes might also be part of the acute phase immune response, by regulating production of key cytokines such as *IL-6* and thus mediating activation of the NF-κB signaling pathways. Nuclear factor (NF)-κB and inhibitor of NF-κB kinase (IKK) proteins regulate innate- and adaptive-immune responses and inflammation (reviewed in [56]). Expression of many of these genes is likely to change as the immune system develops which we will describe in detail in a dedicated network cluster analysis of the GI tract developmental time series dataset. The genes in this cluster therefore appear to be involved both in the onset of rumination and in innate immunity (which could be associated with the population of the rumen microbiome).

Innate and Acquired Immunity

Several clusters exhibited a strong immune signature. Clusters 11, 12, 18, 31 and 32, for example, contained genes with a strong T-lymphocyte signature [57] with high levels of expression in immune cell types and lymphoid tissues. Significantly enriched GO terms for cluster 12, for example, included T-cell differentiation ($p=2.10x10^{-11}$), immune response ($p=0.00182$) and regulation of T-cell activation ($p=0.00019$) (S12 Table). Manual gene annotation using Ensembl IDs within this cluster revealed the majority were T-cell receptors and T-cell surface glycoproteins (S14 Table). Interestingly, ENSOARG00000008993 represents a gene with no orthologues to other species within the Ensembl database, but partial blast hits to T-lymphocyte surface antigen *Ly-9* in mouflon, goat, bison and buffalo in the NCBI database. The 'true' gene LY9, a member of the signalling lymphocyte activation

bioRxiv preprint doi: https://doi.org/10.1101/132696; this version posted June 8, 2017. The copyright holder for this preprint (which was not certified by peer review) is the author/funder. All rights reserved. No reuse allowed without permission.

405 molecule (SLAM) family [58], is also unannotated in sheep and is assigned to
406 ENSOARG00000008981, having multiple orthologues in other placental mammals. We have
407 assigned ENSOARG00000008993 the gene name 'LY9-like' and the symbol *LY9L*, and
408 suggest this transcript plays a role in T-lymphocyte pathogen recognition.

409 Other immune clusters exhibited a macrophage-specific signature, with subsets highly
410 expressed in alveolar macrophages (AMs), monocyte derived macrophages (MDMs) and
411 bone marrow derived macrophages (BMDMs) (cluster 5) and two defined clusters of genes
412 induced in BMDMs stimulated with LPS (cluster 45 and 52). Known macrophage-specific
413 surface markers, receptors and proinflammatory cytokines predominated in these clusters, in
414 addition to numerous unannotated genes, with as yet undefined but probable immune
415 function (S15 Table). For example, the *CD63* antigen, which mediates signal transduction
416 events, was assigned to ENSOARG00000011313 and *BST2* (bone marrow stromal cell
417 antigen 2), which is part of the interferon (IFN) alpha/beta signaling pathway, to
418 ENSOARG00000016787. A third cluster of LPS-inducible genes in macrophages, cluster 64,
419 contained a subset of the IFN-inducible antiviral effector genes, including *DDX58*, *IFIT1*,
420 *IFIT2*, *MX1*, *MX2*, *RSAD2* and *XAF1*, which are induced in mouse and humans through the
421 MyD88-independent *TLR4* signaling pathway via autocrine *IFNB1* signaling (reviewed in
422 [59]). Many other components of this pathway identified in LPS-stimulated human
423 macrophages [60] were either not annotated, or not clustered, and will be the target of
424 detailed annotation efforts in the macrophage dataset.

425 Significantly enriched GO terms for the macrophage-specific cluster 5 included
426 'response to lipopolysaccharide' ($p=7.2x10^{-7}$), and 'toll-like receptor signaling pathway'
427 ($p=3.2x10^{-5}$). Many of the genes in this cluster are known components of the innate immune
428 response in mammals. Interleukin 27 (*IL-27*), is a heterodimeric cytokine which has pro- and
429 anti-inflammatory properties and a diverse effect on immune cells including the regulation of

bioRxiv preprint doi: https://doi.org/10.1101/132696; this version posted June 8, 2017. The copyright holder for this preprint (which was not certified by peer review) is the author/funder. All rights reserved. No reuse allowed without permission.

T-helper cell development, stimulation of cytotoxic T-cell activity and suppression of T-cell proliferation [61]. *ADGRE1* encodes the protein EGF-like module-containing mucin-like hormone receptor-like 1 (*EMR1* also known as F4/80), a classic macrophage marker in mice [62]. Several genes in cluster 5 encode proteins exclusively expressed in macrophages and monocytes. One such gene, *CD163*, encodes a member of the scavenger receptor cysteine-rich (SRCR) superfamily, which protects against oxidative damage by the clearance and endocytosis of hemoglobin/haptoglobin complexes by macrophages, and may also function as an innate immune sensor of bacteria [63].

One of the largest macrophage populations in the body occupies the lamina propria of the small and large intestine [64]. They are so numerous that the expression of macrophage-related genes can be detected within the total mRNA from intestine samples. As noted previously in the pig, one can infer from the expression profiles that certain genes that are highly-expressed in AMs are repressed in the intestinal wall [6]. We proposed that such genes, which included many c-type lectins and other receptors involved in bacterial recognition, were necessary for the elimination of inhaled pathogens, where such responses would be undesirable in the gut [6]. In the sheep, there was no large cohort of receptors that showed elevated expression in AMs relative to MDMs or BMDMs, and that were absent in the gut wall. Only a small cluster (115) of 13 genes showed that profile, including the phagocytic receptor *VSIG4* (CRiG), which is a known strong negative regulator of T-cell proliferation and *IL2* production [65] and *SCIMP*, recently identified as a novel adaptor of Toll-like receptor signaling that amplifies inflammatory cytokine production [66]. Six previously unannotated genes within this small cluster included the E3 ubiquitin ligase, *MARCH1*, and likely members of the paired immunoglobulin type receptor and SIGLEC families, which cannot be definitively assigned as orthologues.

bioRxiv preprint doi: https://doi.org/10.1101/132696; this version posted June 8, 2017. The copyright holder for this preprint (which was not certified by peer review) is the author/funder. All rights reserved. No reuse allowed without permission.

454 Interestingly, macrophage colony-stimulating factor receptor (*CSF1R)*, which
455 controls the survival, proliferation and differentiation of macrophage lineage cells [67, 68],
456 was not within the macrophage-specific cluster 5. Instead, *CSF1R* was in a small cluster
457 (cluster 102) along with several other macrophage-specific genes including the C1Q
458 complex. As in humans and mice [9, 12, 69], *CSF1R* was also expressed in sheep placenta.
459 In humans and mice, placental (trophoblast) expression is directed from a separate promoter
460 [11]. The small number of genes co-expressed with *CSF1R* are likely either co-expressed by
461 trophoblasts as well as macrophages (as is C1Q in humans, see BioGPS
462 (http://biogps.org/dataset/GSE1133/geneatlas-u133a-gcrma/) [9, 70]), or highly-expressed in
463 placenta-associated macrophages.
464
465 **Early Development and Reproduction**
466 The sheep gene expression atlas dataset includes multiple libraries from early
467 developmental time points. Three of the larger clusters of co-expressed genes showed high
468 levels of expression in the fetal ovary (cluster 7), fetal brain (cluster 9) and fetal liver (cluster
469 25). 'Testis-specific' genes, particularly those involved in meiosis and gametogenesis, might
470 also be expressed in the fetal ovary undergoing oogenesis [71, 72]. Our dataset from sheep
471 appears to validate this hypothesis, since genes within cluster 7 exhibited higher levels of
472 expression in the fetal ovary and to a lesser extent the testes. Several genes were expressed
473 both in the testes and the fetal ovary including, testis and ovary specific PAZ domain
474 containing 1 (*TOPAZ1*), which has been shown in sheep to be expressed in adult male testes
475 and in females during fetal development with a peak during prophase I of meiosis [73]. Also,
476 fetal and adult testis expressed 1 (*FATE1*), which is strongly expressed in spermatogonia,
477 primary spermatocytes, and Sertoli cells in seminiferous tubules in mouse and humans [74].
478 Significantly enriched GO terms for genes within cluster 7 included 'female gonad

bioRxiv preprint doi: https://doi.org/10.1101/132696; this version posted June 8, 2017. The copyright holder for this preprint (which was not certified by peer review) is the author/funder. All rights reserved. No reuse allowed without permission.

development' ($p=4.9x10^{-6}$), 'spermatogenesis' ($p=4.6x10^{-8}$) and 'growth factor activity' ($p=5x10^{-5}$) (S12 Table).

Several important genes for embryonic development were also co-expressed in cluster 7. The germ-cell specific gene SRY-box 30 (*SOX30*) encodes a member of the SOX (SRY-related HMG-box) family of transcription factors involved in the regulation of embryonic development and in the determination of cell fate [75]. Growth differentiation factor 3 (GDF3) encodes a protein required for normal ocular and skeletal development. Although it is a major stem cell marker gene [76], it has not previously been linked to germ cell expression. Similarly, POU class 5 homeobox 1 (*POU5F1*) encodes a transcription factor containing a POU homeodomain that controls embryonic development and stem cell pluripotency [76] but is also required for primordial germ cell survival [77]. The expression of these genes in tissues containing germ cells in sheep suggests they contribute to meiosis and cellular differentiation. These observations illustrate the utility of the sheep as a non-human model for the study of gametogenesis.

Cluster 7 also includes two related oocyte-derived members of the transforming growth factor-β (*TGFB1*) superfamily, growth differentiation factor 9 (*GDF9*) and bone morphogenetic protein 15 (*BMP15*), which are essential for ovarian follicular growth and have been shown to regulate ovulation rate and influence fecundity in sheep [78, 79]. Lambing rate is an important production trait in sheep and can vary between breeds based on single nucleotide polymorphism (SNP) mutations in key genes influencing ovulation rate (reviewed in [79, 80]). A number of the known fertility genes in sheep (reviewed in [81, 82]), such as the estrogen receptor (*ESR*) and the Lacaune gene (*B4GALNT2*) were not present in this cluster 7, which may be because they are not expressed in the ovary at the time points chosen for this study. Detailed analysis of the expression of key genes during early development in the fetal ovary in comparison with the ovary from the adult and gestating

bioRxiv preprint doi: https://doi.org/10.1101/132696; this version posted June 8, 2017. The copyright holder for this preprint (which was not certified by peer review) is the author/funder. All rights reserved. No reuse allowed without permission.

ewes may provide additional insights.

Sex Specific Differences in Gene Expression

Sex-specific differences in gene expression have been reported in humans [83, 84] mice [85, 86], cattle [87, 88] and pigs [89, 90]. We examined male and female biased gene expression in the sheep atlas dataset by calculating the average TPM per sex for each gene and the female:male expression ratio (S3 Dataset). Twenty genes exhibited strongly sex biased expression (S16 Table); 13 were female-enriched and 7 were male-enriched. Among the male enriched genes was thyroid stimulating hormone beta (*TSHB*), which is expressed in thyrotroph cells in the pituitary gland and part of a neuro-endocrine signaling cascade in sheep [91]. Expression of *TSHB* in the pituitary gland of male BFxT was 3.6-fold higher than in female BFxT sheep. A similar sex bias has been observed in rats in which males exhibit significantly higher *TSHB* expression in the pituitary gland than females [92].

Other genes exhibiting similarly large sex specific fold-changes included keratin 36 (*KRT36*) which was expressed 6.6-fold higher in the reticulum of male relative to female sheep and *VSIG1* (V-Set and immunoglobulin domain containing 1), which is required for the differentiation of glandular gastric epithelia [93]. *VSIG1* showed 4-fold greater expression in the female pylorus relative to the male. An unannotated gene ENSOARG00000020792 exhibited large fold change in male biased expression in immune tissues including popliteal and prescapular lymph node, tonsil and Peyer's patch. This gene has a detectable blast hit to "immunoglobulin kappa-4 light chain variable region" and is a 1:1 orthologue with an unannotated gene in cattle, ENSBTAG00000045514, with ≥70% reciprocal percentage identity and conservation of synteny. The dN/dS for ENSOARG00000020792 suggests it is evolving rapidly (dN/dS > 2). Male-biased genes are known to evolve quickly, as are immune genes [94]. GO term enrichment for the set of genes with five-fold sex-biased expression in

bioRxiv preprint doi: https://doi.org/10.1101/132696; this version posted June 8, 2017. The copyright holder for this preprint (which was not certified by peer review) is the author/funder. All rights reserved. No reuse allowed without permission.

529 at least one BFxT tissue (S17 Table) revealed that the genes enriched in females were
530 predominately involved with the immune reponse while gene enriched in the male were
531 broadly associated with muscle and connective tissue. This is likely to reflect inherent
532 differences between the two sexes in allocation of resources towards growth or immunity.
533 Genes exhibiting sex specific expression might therefore be relevant in sexual diamorphism
534 in disease susceptibility for example, and warrant further investigation.
535
536 **Differential Expression of Genes between the Texel and BFxT**
537 The majority of commercially-produced livestock are a cross of two or more different
538 production breeds with distinct desired traits [95]. For example, in the UK, the crossing of
539 lighter upland sheep breeds with heavier lowland meat breeds optimises carcass quality,
540 lambing rate, growth rate and survivability [95]. In developing countries, sustainable crossing
541 of indigenous small ruminants with elite western breeds is one approach to improve
542 productivity [96, 97]. An RNA-Seq dataset of this size from an outbred cross of two disparate
543 sheep breeds provides an opportunity to investigate differential gene expression in a purebred
544 parental line and crossbred animals. We compared gene expression across tissues in the F_1
545 crossbred (BFxT) animals (generated by crossing a Texel ram with a Scottish Blackface ewe;
546 Fig 5A) with the purebred Texel animals included in the previous sheep gene expression atlas
547 dataset [18].
548 A gene was considered differentially expressed (DE) between the purebred Texel and
549 hybrid BFxT if (a) it was expressed at ≥1 TPM in both Texel and BFxT (considering TPM to
550 be the mean of all replicates per tissue), (b) the fold change (ratio of BFxT TPM to Texel
551 TPM) was ≥2 in ≥25% of the tissues in which expression was detected (stipulating no
552 minimum number of tissues, but noting that 23 tissues are common to Texel and BFxT), and
553 (c) the fold change was ≥5 in at least 1 tissue. Fold changes of all genes expressed at ≥1 TPM

bioRxiv preprint doi: https://doi.org/10.1101/132696; this version posted June 8, 2017. The copyright holder for this preprint (which was not certified by peer review) is the author/funder. All rights reserved. No reuse allowed without permission.

554 in both breeds are given in S18 Table. The GO terms enriched in the set of DE genes (n=772)
555 with higher expression in the BFxT than the Texel were predominantly related either to
556 muscle or brain function (S19 Table). The top 20 genes showing the largest up-regulation
557 (shown as absolute fold-change) in the BFxT relative to the purebred Texel sheep are
558 illustrated in Fig 5B. Enriched molecular function GO terms for the set of genes differentially
559 expressed between BFxT and Texel sheep include 'iron ion binding' ($p=3.6x10^{-4}$), and
560 'cytoskeletal protein binding' ($p=7.8x10^{-6}$), biological process terms include 'cellular iron ion
561 homeostasis' ($p=6.3x10^{-4}$) and cellular component terms include 'sarcomere' ($p=6.6x10^{-7}$) and
562 'collagen trimer' ($p=5.5x10^{-7}$) (S19 Table).

563 Numerous genes with structural, motor and regulatory functions were highly
564 expressed in BFxT compared to Texel bicep muscle, with approximately 5- to 18-fold
565 expression increases for various members of the collagen (*COL1A1*, *COL1A2*, *COL3A1*) and
566 myosin families (*MYH2*, *MYL4*), along with *CSRP3* (a mechanosensor) [98], *FMOD*
567 (fibromodulin, a regulator of fibrillogenesis) [99], keratocan (*KERA*, a proteoglycan involved
568 in myoblast differentiation) [100], matrix metalloproteinase 2 (*MMP2*, a proteolytic enzyme
569 associated with muscle regeneration) [101], and calsequestrin 2 (*CASQ2*, one of the most
570 abundant Ca^{2+}-binding proteins in the sarcoplasmic reticulum, essential for muscle
571 contraction) [102].

572 Genes enriched in muscle are of particular biological and commercial interest because
573 Texel sheep exhibit enhanced muscling and less fat [103], due to a single nucleotide
574 polymorphism (SNP) in the 3' untranslated region of the myostatin gene *MSTN* (synonym
575 *GDF-8*) which generates an illegitimate miRNA binding site resulting in translational
576 inhibition of myostatin synthesis and contributing to muscular hypertrophy [24, 104].
577 Because heterozygotes have an intermediate phenotype, cross breeding of homozygous
578 mutant Texel sheep with animals homozygous for the normal allele transmits something of

bioRxiv preprint doi: https://doi.org/10.1101/132696; this version posted June 8, 2017. The copyright holder for this preprint (which was not certified by peer review) is the author/funder. All rights reserved. No reuse allowed without permission.

579 the Texel muscle phenotype to the offspring. An effect on muscle synthesis in the BFxT
580 animals could be related to the myostatin genotype; genes with higher expression in the Texel
581 than in the cross may be targets for myostatin inhibition [105], while those with lower
582 expression in the Texel than in the cross may be directly or indirectly activated by myostatin
583 and hence involved in the cessation of muscle differentiation. In cattle the myostatin mutation
584 is associated with the downregulation of collagen genes including *COL1A1* and *COL1A2*
585 [105]. This is consistent with the observation that these genes have higher expression in the
586 heterozygous BFxT animals than the Texel animals. Since myostatin also regulates muscle
587 fibre type [106] by suppressing the formation of fast-twitch fibres, individuals homozygous
588 for inactivating myostatin mustations are likely to exhibit increased fast-twitch fibres [107].
589 Many of the genes up-regulated in the BFxT relative to the Texel animals (e.g. *CSRP3* and
590 *CASQ2*) are known to be specifically expressed in slow-twitch muscle [106, 108], and
591 several down-regulated genes are associated with fast-twitch muscle (e.g. *TNNC2, TNNI2*
592 and *SERCA1*) [109, 110]. Consequently, the difference between the cross-breed and pure
593 Texel is in part attributable to an increased contribution of slow-twitch fibres, which in turn
594 has been associated with desirable meat quality traits [111] highlighting the potential
595 advantages of cross-breeding.

596 Enriched GO terms related to brain function include the 'myelin sheath' ($p=6.1x10^{-8}$)
597 and the 'internode region of the axon' ($p=5.2x10^{-5}$) (S19 Table). Candidate genes of
598 particular interest were expressed in the cerebellum (S18 Table). For instance, in the BFxT
599 relative to the Texel animals, there were approximately 8-fold expression increases in cochlin
600 (*COCH*, which regulates intraocular pressure) [112] and brevican (*BCAN*, functions
601 throughout brain development in both cell-cell and cell-matrix interactions) [113, 114] and a
602 10-fold expression increase for myelin-associated oligodendrocyte basic protein, MOBP,
603 which was previously unannotated in sheep (ENSOARG00000002491) and has a function in

bioRxiv preprint doi: https://doi.org/10.1101/132696; this version posted June 8, 2017. The copyright holder for this preprint (which was not certified by peer review) is the author/funder. All rights reserved. No reuse allowed without permission.

late-stage myelin sheath compaction [115]. A 15-fold expression increase was observed for oligodendrocytic paranodal loop protein (*OPALIN*, a transmembrane protein unique to the myelin sheath [116]), in the BFxT relative to the Texel and a 10-fold increase for another unannotated gene myelin basic protein (*MBP*), which we have assigned to ENSOARG00000004374 [117]. Although these examples of a neuroendocrine-specific effect of cross-breeding are speculative, they are of interest as Scottish Blackface sheep exhibit both improved neonatal behavioural development [118] and more extensive foraging behaviour than lowland breeds such as the Texel, travelling further distances, covering greater areas and exploring higher altitudes [119].

Visualisation of the Expression Atlas

We have provided the BFxT sheep gene expression atlas as a searchable database in the gene annotation portal BioGPS (http://biogps.org/dataset/BDS_00015/sheep-atlas/). By searching the dataset via the following link (http://biogps.org/sheepatlas/) the expression profile of any given gene can be viewed across tissues. An example profile of the *MSTN* (*GDF-8*) myostatin gene from sheep is included in Fig 6. BioGPS allows comparison of expression profiles across species and links to gene information for each gene [70, 120, 121]. The Sheep Atlas BioGPS expression profiles are based on TPM estimates from the alignment-free Kallisto output for the BFxT libraries, averaged across samples from each developmental stage for ease of visualisation. It is important to note that there may be a degree of variation in the expression pattern of individual genes between individuals which is masked when the average profiles are displayed. In addition, to allow comparison between species BioGPS requires each gene have an Entrez ID, which is not the case for all genes in Oar v3.1 and as a consequence these genes do not have visualisable expression profiles in

bioRxiv preprint doi: https://doi.org/10.1101/132696; this version posted June 8, 2017. The copyright holder for this preprint (which was not certified by peer review) is the author/funder. All rights reserved. No reuse allowed without permission.

BioGPS. The expression profiles of the genes without Entrez IDs can be found in S1 Dataset and S2 Dataset.

In parallel to the alignment-free Kallisto method, we also used an alignment-based approach to RNA-Seq processing, with the HISAT aligner [122] and StringTie assembler [123] (detailed in S1 Methods). These alignments will be published as tracks in the Ensembl genome browser in the short term and integrated into the next Ensembl genome release for sheep.

Conclusions

This work describes the transcriptional landscape of the sheep across all major organs and multiple developmental stages, providing the largest gene expression dataset from a livestock species to date. The diversity of samples included in the sheep transcriptional atlas is the greatest from any mammalian species, including humans. Livestock provide an attractive alternative to rodents as models for human conditions in that they are more human-like in their size, physiology and transcriptional regulation, as well as being economically important in their own right. Non-human models are required to study the fundamental biology of healthy adult mammals and as such this dataset represents a considerable new resource for understanding the biology of mammalian tissues and cells.

In this sheep transcriptional atlas gene expression was quantified at the gene level across a comprehensive set of tissues and cell-types, providing a starting point for assigning function based on cellular expression patterns. We have provided functional annotation for hundreds of genes that previously had no meaningful gene name using co-expression patterns across tissues and cells. Future analysis of this dataset will use the co-expression clusters to link gene expression to observable phenotypes by highlighting the expression patterns of candidate genes associated with specific traits from classical genetic linkage studies or

bioRxiv preprint doi: https://doi.org/10.1101/132696; this version posted June 8, 2017. The copyright holder for this preprint (which was not certified by peer review) is the author/funder. All rights reserved. No reuse allowed without permission.

genome-wide association studies (GWAS). Gene expression datasets have been used in this way to characterise cell populations in mouse [22, 23] and in the biological discovery of candidate genes for key traits in sheep [124-126] and pigs [127, 128]. We have already utilised the dataset to examine the expression patterns of a set of candidate genes linked to mastitis resistance [129] in sheep, including comparative anlaysis with a recently available RNA-Seq dataset from sheep lactating mammary gland and milk samples [130]. The research community will now be able to use the sheep gene expression atlas dataset to examine the expression patterns of their genes or systems of interest, to answer many of the outstanding questions in ruminant biology, health, welfare and production.

Improving the functional annotation of livestock genomes is critical for biological discovery and in linking genotype to phenotype. The Functional Annotation of Animal Genomes Consortium (FAANG) aims to establish a data-sharing and research infrastructure capable of analysing efficiently genome wide functional data for animal species [26, 27]. This analysis is undertaken on a large scale, including partner institutions from across the globe, to further our understanding of how variation in gene sequences and functional components shapes phenotypic diversity. Analysis of these data will improve our understanding of the link between genotype and phenotype, contribute to biological discovery of genes underlying complex traits and allow the development and exploitation of improved models for predicting complex phenotypes from sequence information. The sheep expression atlas is a major asset to genome assembly and functional annotation and provide the framework for interpretation of the relationship between genotype and phenotype in ruminants.

Methods

Animals

bioRxiv preprint doi: https://doi.org/10.1101/132696; this version posted June 8, 2017. The copyright holder for this preprint (which was not certified by peer review) is the author/funder. All rights reserved. No reuse allowed without permission.

678 Approval was obtained from The Roslin Institute's and the University of Edinburgh's
679 Protocols and Ethics Committees. All animal work was carried out under the regulations of
680 the Animals (Scientific Procedures) Act 1986. Three male and three female Scottish
681 Blackface x Texel sheep of approximately two years of age were acquired locally and housed
682 indoors for a 7-10 day "settling-in period" prior to being euthanased (electrocution and
683 exsanguination). Nine Scottish Blackface x Texel lambs were born at Dryden Farm Large
684 Animal Unit. Three neonatal lambs were observed at parturition and euthanised immediately
685 prior to their first feed, three lambs were euthanised at one week of age prior to rumination
686 (no grass was present in their GI tract) and three at 8 weeks of age once rumination was
687 established. The lambs were euthanised by schedule one cranial bolt. To obtain
688 developmental tissues six Scottish Blackface ewes were mated to a Texel ram and scanned to
689 ensure successful pregnancy at 21 days. Two were euthanised at 23 days, two at 35 days and
690 two at 100 days gestation (electrocution followed by exsanguination). Corresponding time
691 points (day 23, 35 and 100) from gestating BFxT ewes mated with a Texel ram and
692 euthanised as for the Blackface ewes were also included. All the animals, were fed *ad libitum*
693 on a diet of hay and 16% sheep concentrate nut, with the exception of the lambs pre-weaning
694 who suckled milk from their mothers. Details of the animals sampled are included in S1
695 Table.
696
697 **Tissue Collection**
698 Tissues (95 tissues/female and 93 tissues/male) and 5 cell types were collected from
699 three male and three female adult Scottish Blackface x Texel (BFxT) sheep at two years of
700 age. The same tissues were collected from nine lambs, 3 at birth, 3 at one week and 3 at 8
701 weeks of age. Three embryonic time points were also included: three day-23 BFxT whole
702 embryos, three BFxT day 35 embryos from which tissue was collected from each region of

bioRxiv preprint doi: https://doi.org/10.1101/132696; this version posted June 8, 2017. The copyright holder for this preprint (which was not certified by peer review) is the author/funder. All rights reserved. No reuse allowed without permission.

703 the basic body plan and three day 100 BFxT embryos from which 80 tissues were collected.
704 Reproductive tissue from the corresponding time points from 6 BFxT ewes, 2 at each
705 gestational time point, was also collected. In addition, 3 pools of 8 day 7 blastocysts from
706 abattoir derived oocytes (of unknown breed) fertilized with Texel semen were created using
707 IVF.

708 The majority of tissue samples were collected into RNAlater (AM7021; Thermo
709 Fisher Scientific, Waltham, USA) and a subset were snap frozen, including lipid rich tissues
710 such as adipose and brain. To maintain RNA integrity all tissue samples were harvested
711 within an hour from the time of death. A detailed list of the tissues collected and sequenced
712 can be found in S2 Table. Within the scope of the project we could not generate sequence
713 data from all the samples collected and have archived the remainder for future analysis.
714 Sample metadata, conforming to the FAANG Consortium Metadata standards, for all the
715 samples collected for the sheep gene expression atlas project has been deposited in the
716 BioSamples database under project identifier GSB-718
717 (https://www.ebi.ac.uk/biosamples/groups/SAMEG317052).

718

719 **Isolation of Cell Types**

720 All cell types were isolated on the day of euthanasia. Bone marrow cells were isolated
721 from 10 posterior ribs as detailed for pig [131]. BMDMs were obtained by culturing bone
722 marrow cells for 7 days in complete medium: RPMI 1640, Glutamax supplement (35050-61;
723 Invitrogen, Paisley, U.K.), 20% sheep serum (S2263; Sigma Aldrich, Dorset, U.K),
724 penicillin/streptomycin (15140; Invitrogen) and in the presence of recombinant human CSF-1
725 (rhCSF-1: 10^4 U/ml; a gift of Chiron, Emeryville, CA) on 100-mm^2 sterile petri dishes,
726 essentially as described previously for pig [131]. For LPS stimulation the resulting
727 macrophages were detached by vigorous washing with medium using a syringe and 18-g

bioRxiv preprint doi: https://doi.org/10.1101/132696; this version posted June 8, 2017. The copyright holder for this preprint (which was not certified by peer review) is the author/funder. All rights reserved. No reuse allowed without permission.

728 needle, washed, counted, and seeded in tissue culture plates at 10^6 cells/ml in CSF-1–
729 containing medium. The cells were treated with LPS from *Salmonella enterica* serotype
730 minnesota Re 595 (L9764; Sigma-Aldrich) at a final concentration of 100 ng/ml as
731 previously described in pig [131] and harvested into TRIzol® (Thermo Fisher Scientific) at 0,
732 2, 4, 7 and 24 h post LPS treatment before storing at -80°C for downstream RNA extraction.
733 PBMCs were isolated as described for pig [132]. MDMs were obtained by culturing
734 PBMCs for 7 days in CSF-1–containing medium, as described above for BMDMs, and
735 harvesting into TRIzol® (Thermo Fisher Scientific). Alveolar macrophages were obtained by
736 broncho-alveolar lavage of the excised lungs with 500ml sterile PBS (Mg^{2+} Ca^{2+} free)
737 (P5493; Sigma Aldrich). The cells were kept on ice until processing. To remove surfactant
738 and debris cells were filtered through 100uM cell strainers and centrifuged at 400 × *g* for 10
739 min. The supernatant was removed and 5ml red blood cell lysis buffer (420301**;** BioLegend,
740 San Diego, USA) added to the pellet for 5 min; then the cells were washed in PBS (Mg^{2+}
741 Ca^{2+} free) (P5493; Sigma Aldrich) and centrifuged at 400 × *g* for 10 min. The pellet was
742 collected, resuspended in sterile PBS (Mg^{2+} Ca^{2+} free) (Sigma Aldrich), and counted.
743 Alveolar macrophages were seeded in 6-well tissue culture plates in 2ml complete medium:
744 RPMI 1640, Glutamax supplement (35050-61; Invitrogen), 20% sheep serum (S2263; Sigma
745 Aldrich), penicillin/streptomycin (15140; Invitrogen) in the presence of rhCSF1 (10^4 U/ml)
746 overnight.
747 Blood leukocytes were isolated as described in [133]. Whole blood was spun at 500 x
748 *g* for 10 min (no brake) to separate the buffy coats. These were then lysed in ammonium
749 chloride lysis buffer (150mM NH_4Cl, 10mM $NaHCO_3$, 0.1mM EDTA) for 10 min on a
750 shaking platform, then centrifuged at 4°C for 5 min at 500 x *g*. The resultant blood leukocyte
751 pellets were stored in 1ml of RNAlater (Thermo Fisher Scientific) at -80°C.

bioRxiv preprint doi: https://doi.org/10.1101/132696; this version posted June 8, 2017. The copyright holder for this preprint (which was not certified by peer review) is the author/funder. All rights reserved. No reuse allowed without permission.

To isolate embryonic fibroblasts we harvested a day 35 embryo whole and transferred to outgrowth media (DMEM, high glucose, glutamine, pyruvate (Thermo Fisher Scientific; 11995065), FBS (Fetal Bovine Serum) (Thermo Fisher Scientifc; 10500056), MEM NEAA (Thermo Fisher Scientific; 11140068), penicillin/streptomycin (Invitrogen), Fungizone (Amphotericin B; Thermo Fisher Scientific; 15290018), Gentamicin (Thermo Fisher Scientific; 15750037)). In a sterile flow hood the head was removed and the body cavity eviscerated. The remaining tissue was washed 3 times in PBS (Mg^{2+} Ca^{2+} free) (Sigma Aldrich) with penicillin/streptomycin (Invitrogen). 5ml of Trypsin-EDTA solution (T4049; Sigma Aldrich) was added and the sample incubated at 37°C for 5 min then vortexed and incubated for an additional 5min at 37°C. 3ml of solution was removed and filtered through a 100uM cell strainer, 5ml of outgrowth media was then passed through the strainer and combined with the sample. The sample was centrifuged at 200 x *g* for 3 min and the pellet resuspended in 9ml of out growth media before splitting the sample between 3x T75 flasks. The process then was repeated for remaining 2ml of sample left after the digestion with Trypsin (above). Embryonic fibroblasts were incubated for 5-7 days (until 80-90% confluent) then harvested into TRIzol® Reagent (Thermo Fisher Scientific).

RNA Extraction and Library Preparation

RNA was extracted using the same method as the Roslin RNA-Seq samples included in the sheep genome project detailed in [18]. For each RNA extraction <100mg of tissue was processed. Care was taken to ensure snap frozen samples remained frozen prior to homogenisation, and any cutting down to the appropriate size was carried out over dry ice. Tissue samples were first homogenised in 1ml of TRIzol® reagent (15596018; Thermo Fisher Scientific) with either CK14 (432-3751; VWR, Radnor, USA) or CKMIX (431-0170; VWR) tissue homogenising ceramic beads on a Precellys® Tissue Homogeniser (Bertin Instruments; Montigny-le-Bretonneux, France). Homogenisation conditions were optimised for tissue type

bioRxiv preprint doi: https://doi.org/10.1101/132696; this version posted June 8, 2017. The copyright holder for this preprint (which was not certified by peer review) is the author/funder. All rights reserved. No reuse allowed without permission.

but most frequently 5000 rpm for 20 sec. Cell samples which had previously been collected in TRIzol® Reagent (15596018; Thermo Fisher Scientific), were mixed by pipetting to homogenise. Homogenised (cell/tissue) samples were then incubated at room temperature for 5 min to allow complete dissociation of the nucleoprotein complex, 200µl BCP (1-bromo-3-chloropropane) (B9673; Sigma Aldrich) was added, then the sample was shaken vigorously for 15 sec and incubated at room temperature for 3 min. The sample was centrifuged for 15 min at 12,000 x *g*, at 4°C to separate the homogentate into a clear upper aqueous layer (containing RNA), an interphase and red lower organic layers (containing the DNA and proteins), for three min. DNA and trace phenol was removed using the RNeasy Mini Kit (74106; Qiagen Hilden, Germany) column purification, following the manufacturers instructions (Protocol: Purification of Total RNA from Animal Tissues, from step 5 onwards). RNA quantity was measured using a Qubit RNA BR Assay kit (Q10210; Thermo Fisher Scientific) and RNA integrity estimated on an Agilent 2200 Tapestation System (Agilent Genomics, Santa Clara, USA) using the RNA Screentape (5067-5576; Agilent Genomics) to ensure RNA quality was of $RIN^e > 7$.

RNA-Seq libraries were prepared by Edinburgh Genomics (Edinburgh Genomics, Edinburgh, UK) and run on the Illumina HiSeq 2500 sequencing platform (Illumina, San Diego, USA). Details of the libraries generated can be found in S2 Table. A subset of 10 tissue samples and BMDMs at 0 h and 7h (+/-LPS) (Table 1), from each individual, were sequenced at a depth of >100 million strand-specific 125bp paired-end reads per sample using the standard Illumina TruSeq total RNA library preparation protocol (Ilumina; Part: 15031048, Revision E). These samples were chosen to include the majority of transcriptional output, as in [134]). An additional 40 samples from the tissues and cell types collected per individual (44/female and 42/male), were selected and sequenced at a depth of >25 million

bioRxiv preprint doi: https://doi.org/10.1101/132696; this version posted June 8, 2017. The copyright holder for this preprint (which was not certified by peer review) is the author/funder. All rights reserved. No reuse allowed without permission.

802 strand-specific paired-end reads per sample using the standard Illumina TruSeq mRNA
803 library preparation protocol (poly-A selected) (Ilumina; Part: 15031047 Revision E).

804 In addition to the samples from the 6 adults, tissue was also collected from other
805 developmental time points. The GI tract tissues collected from the 9 BFxT lambs, 3 at birth, 3
806 at one week of age and 3 at 8 weeks of age were sequenced at a depth of >25 million reads
807 per sample using the Illumina mRNA TruSeq library preparation protocol (poly-A selected)
808 as above. Of the early developmental time points, the three 23 day old embryos from BFxT
809 sheep were sequenced at >100 million reads using the Illumina total RNA TruSeq library
810 preparation protocol (as above), while the other embryonic samples and the ovary and
811 placenta from the gestating ewes were sequenced at a depth of >25 million reads per sample
812 using the Illumina mRNA TruSeq library preparation protocol (as above). In addition, three
813 libraries were generated using the NuGen Ovation Single Cell RNA-Seq System (0342-32-
814 NUG; NuGen, San Carlos, USA) from pooled samples of 8 blastocysts (as in [135]), and
815 sequenced at a depth of >60 million reads per sample. A detailed list of prepared libraries,
816 including library type can be found in S2 Table.

817 To identify spurious samples we used sample-to-sample correlation, of the transposed
818 data from S1 Dataset, in Miru (Kajeka Ltd) [37]. The sample-to-sample graph is presented in
819 S2 Fig. The expression profiles of any samples clustering unexpectedly (i.e. were not found
820 within clusters of samples of the same type/biological replicate) were examined in detail.
821 Generally the correlation between samples was high, although 4 spurious samples and 4 sets
822 of swapped samples were identified. These samples were either relabeled or removed as
823 appropriate.

824

825 **Data Quality Control and Processing**

bioRxiv preprint doi: https://doi.org/10.1101/132696; this version posted June 8, 2017. The copyright holder for this preprint (which was not certified by peer review) is the author/funder. All rights reserved. No reuse allowed without permission.

826 Raw data is deposited in the European Nucleotide Archive under study accession
827 number PRJEB19199 (http://www.ebi.ac.uk/ena/data/view/PRJEB19199). The RNA-Seq
828 data processing methodology and pipelines are described in detail in S1 Methods. For each
829 tissue a set of expression estimates, as transcripts per million (TPM), were obtained using the
830 high speed transcript quantification tool Kallisto [29]. In total, the expression atlas utilised
831 approximately 26 billion (pseudo) alignments (S3 Table), capturing a large proportion of
832 protein-coding genes per tissue (S20 Table).

833 The accuracy of Kallisto is dependent on a high quality index (reference
834 transcriptome) [29], so in order to ensure an accurate set of gene expression estimates we
835 employed a 'two-pass' approach. We first ran Kallisto on all samples using as its index the
836 Oar v3.1 reference transcriptome. We then parsed the resulting data to revise this index. This
837 was in order to include, in the second index, those transcripts that should have been there but
838 were not (i.e. where the reference annotation is incomplete), and to remove those transcripts
839 that should not be there but were (i.e. where the reference annotation is poor quality and a
840 spurious model has been introduced). For the first criterion, we obtained the subset of reads
841 that Kallisto could not align, assembled those *de novo* into putative transcripts (S1 Methods),
842 then retained each transcript only if it could be robustly annotated (by, for instance, encoding
843 a protein similar to one of known function) and showed coding potential (S21 Table). For the
844 second criterion, we identified those members of the reference transcriptome for which no
845 evidence of expression could be found in any of the hundreds of samples comprising the
846 atlas. These were then discarded from the index. Finally, this revised index was used for a
847 second iteration of Kallisto, generating higher-confidence expression level estimates. This
848 improved the capture rate of protein-coding genes (S22 Table). A detailed description of this
849 process can be found in S1 Methods.

bioRxiv preprint doi: https://doi.org/10.1101/132696; this version posted June 8, 2017. The copyright holder for this preprint (which was not certified by peer review) is the author/funder. All rights reserved. No reuse allowed without permission.

We complemented this alignment-free method with a conventional alignment-based approach to RNA-Seq processing, using the HISAT aligner [122] and StringTie assembler [123]. A detailed description of this pipeline is included in S1 Methods. This assembly is highly accurate with respect to the existing (Oar v3.1) annotation, precisely reconstructing almost all exon (96%), transcript (98%) and gene (99%) models (S23 Table). Although this validates the set of transcripts used to generate the Kallisto index, we did not use HISAT/StringTie to quantify expression. This is because a standardised RNA space is necessary to compare data from mRNA-Seq and total RNA-Seq libraries [31], which cannot be applied if expression is quantified via genomic alignment. Unlike alignment-free methods, however, HISAT/StringTie can be used to identify novel transcript models (S24 Table), particularly for ncRNAs, which will be described in detail in a dedicated analysis. We will publish the alignments from HISAT and Stringtie as tracks in the Ensembl genome browser in the short term and integrate the alignments into Ensembl and Biomart in the next Ensembl release for sheep.

Inclusion of Additional RNA-Seq Datasets from Sheep

Additional RNA-Seq data was obtained from a previous characterisation of the transcriptome of 3 Texel sheep included in the release of the current sheep genome Oar v3.1 [18]. The dataset included tissues from an adult Texel ram (n=29), an adult Texel ewe (n=25) and their female (8-9 month old) lamb (n=28), plus a whole embryo (day 15 gestation) from the same ram-ewe pairing. The raw read data from the 83 Texel samples incorporated into this dataset and previously published in [18] is located in the European Nucleotide Archive (ENA) study accession PRJEB6169 (http://www.ebi.ac.uk/ena/data/view/PRJEB6169). The metadata for these individuals is included in the BioSamples database under Project Identifier GSB-1451 (https://www.ebi.ac.uk/biosamples/groups/SAMEG317052). A small proportion

bioRxiv preprint doi: https://doi.org/10.1101/132696; this version posted June 8, 2017. The copyright holder for this preprint (which was not certified by peer review) is the author/funder. All rights reserved. No reuse allowed without permission.

of the tissues included in the Texel RNA-Seq dataset were not sampled in the BFxT gene expression atlas. Those unique to the Texel are largely drawn from the female reproductive, integument and nervous systems: cervix, corpus luteum, ovarian follicles, hypothalamus, brain stem, omentum and skin (side and back). Details of the Texel RNA-Seq libraries including tissue and cell type are included in S25 Table. The Texel samples were all prepared using the Illumina TruSeq stranded total RNA protocol with the Ribo-Zero Gold option for both cytoplasmic and mitochondrial rRNA removal, and sequenced using the Illumina HiSeq 2500 (151bp paired-end reads) [18]. As above, Kallisto was used to estimate expression level for all samples, using the revised reference transcriptome (from the 'second pass') as its index.

Correcting for the Effect of Multiple Library Types

To correct for the confounding effect of multiple library types we applied a batch effect correction. We have previously validated this method using a subset of the sheep atlas expression atlas samples from BMDMs (+/- LPS) sequenced both as mRNA and total RNA libraries [31]. As described above, for the Kallisto second pass, we constrained the Kallisto index to contain only the transcripts of protein-coding genes, pseudogenes and processed pseudogenes, the majority of which are poly(A)+ and so are present in both mRNA-Seq and total RNA-Seq samples. We then calculated, per gene, the ratio of mean TPM across all mRNA-Seq libraries to mean TPM across all total RNA-Seq libraries. Given the scope of the tissues sampled for both library types (all major organ systems from both sexes and from different developmental states), neither mean is likely to be skewed by any tissue-specificity of expression. As such, any deviations of this ratio from 1 will reflect variance introduced by library type/depth. Thus, to correct each gene's set of expression estimates for this effect of library type, we multiplied all total RNA-Seq TPMs by this ratio. To validate this approach

bioRxiv preprint doi: https://doi.org/10.1101/132696; this version posted June 8, 2017. The copyright holder for this preprint (which was not certified by peer review) is the author/funder. All rights reserved. No reuse allowed without permission.

we used principal component bi-plot analysis, described and shown in S1 Methods and S1 Fig.

Gene Expression, Network Cluster Analysis and Annotation

Network cluster analysis of the sheep gene expression atlas was performed using Miru (Kajeka Ltd, Edinburgh, UK) [35-37]. In brief, similarities between individual gene expression profiles were determined by calculating a Pearson correlation matrix for both gene-to-gene and sample-to-sample comparisons, and filtering to remove relationships where $r < 0.75$. A network graph was constructed by connecting the remaining nodes (genes) with edges (where the correlation exceeded the threshold value). This graph was interpreted by applying the Markov Cluster algorithm (MCL) [38] at an inflation value (which determines cluster granularity) of 2.2. The local structure of the graph was then examined visually. Genes with robust co-expression patterns, implying related functions, clustered together, forming cliques of highly interconnected nodes. A principle of 'guilt by association' was then applied, i.e. the function of an unannotated gene could be inferred from the genes it clustered with [20, 136]. Expression profiles for each cluster were examined in detail to understand the significance of each cluster in the context of the biology of sheep tissues and cells. Clusters 1 to 50 (Table 2) were assigned a functional 'class' and 'sub-class' manually by first determining if multiple genes within a cluster shared a similar biological function based on both gene ontology [39], determined using the Bioconductor package 'topGO' [137] (GO term enrichment for clusters 1 to 50 is shown in S12 Table). We then compared the clusters with tissue- and cell-specific clusters in other large-scale network-based gene expression analyses including the pig gene expression atlas [6], the human protein atlas [69, 72, 138] and the mouse atlas [9, 139, 140]. More specific annotation of the GI tract clusters in sheep was

bioRxiv preprint doi: https://doi.org/10.1101/132696; this version posted June 8, 2017. The copyright holder for this preprint (which was not certified by peer review) is the author/funder. All rights reserved. No reuse allowed without permission.

based on network and pathway analysis from the sheep genome paper and a subsequent satellite publication [18, 21]. The gene component of all clusters can be found in S11 Table.

We assigned gene names to unnannotated genes in Oar v3.1 based on their co-expression pattern, tissue specificity, and reciprocal percent identity to a set of nine known ruminant proteomes (S7 Table). The annotation pipeline is described in detail in S1 Methods and included a set of quality categories summarised in S5 Table. We were able to assign gene names to >1000 previously unannotated genes in Oar v3.1. Candidate gene names are given as both a shortlist (S8 Table) and a longlist (S9 Table), the latter intended for manual review as informative annotations may still be made without every one of the above criteria being met.

Abbreviations

AM, Alveolar Macrophage; BFxT, Scottish Blackface x Texel; BMDM, Bone Marrow Derived Macrophage; CNS, Central Nervous System; DE, Differential Expression; EBI, European Bioinformatics Institute; ENA, European Nucleotide Archive; FAANG, Functional Annotation of ANimal Genomes; GI, Gastrointestinal; HGNC, HUGO (Human Genome Organisation) Gene Nomenclature Committee; LPS, Lipopolysaccharide; MCL, Markov Cluster Algorithm; MCLi, Markov Cluster Algorithm Inflation; MDM, Monocyte Derived Macrophage; mRNA, messenger Ribonucleic Acid; NF-κB, Nuclear Factor Kappa-Light-Chain-Enhancer of Activated B-Cells; PBMC, Peripheral Blood Mononuclear Cell; RNA-Seq, RNA Sequencing; PPAR, Peroxisome Proliferator-Activated Receptor; rhCSF1, Recombinant Human Colony Stimulating Factor 1; SIGLEC, Sialic Acid-Binding Immunoglobulin-Like Lectin; SNP, Single Nucleotide Polymorphism

Acknowledgments

bioRxiv preprint doi: https://doi.org/10.1101/132696; this version posted June 8, 2017. The copyright holder for this preprint (which was not certified by peer review) is the author/funder. All rights reserved. No reuse allowed without permission.

We would like to thank the large number of people at the Roslin Institute who helped with the many aspects of the sheep atlas project. Douglas McGavin and David Chisholm coordinated the management of the sheep at Dryden Farm. Tim King, Peter Tennant, Adrian Ritchie, John Bracken and Pip Beard conducted post mortems on the animals. The lists of tissues for collection were developed by Erika Abbondati. Detailed dissection of the brain was performed by Fiona Houston. The tissue collection team included Heather Finlayson, Christine Burkhard, Alison Wilson, Ailsa Carlisle, Mark Barnett, Gemma Davis, Anna Raper, Rocio Rojo, Alex Brown, Chris Proudfoot, Laura Glendinning, Sara Clohisey, Yolanda Corripio-Miyar, Jack Ferguson, Karen Fernie and Jason Ioannidis. Blood Leukocytes were isolated by John Hopkins. RNA from the GI Tract was isolated by Gemma Davis and from embryonic fibroblasts by Charity Muriuki. Library preparation and sequencing was carried out by Edinburgh Genomics, The University of Edinburgh. We would also like to thank Norman Russell (The Roslin Institute) for generating the photographic images used and Andrew Su for allowing us to use BioGPS as the platform for visualistion of the expression data.

References

1. Marino R, Atzori AS, D'Andrea M, Iovane G, Trabalza-Marinucci M, Rinaldi L. Climate change: Production performance, health issues, greenhouse gas emissions and mitigation strategies in sheep and goat farming. Small Ruminant Research. 2016;135:50-9. doi: doi.org/10.1016/j.smallrumres.2015.12.012.

2. Brito LF, Clarke SM, McEwan JC, Miller SP, Pickering NK, Bain WE, et al. Prediction of genomic breeding values for growth, carcass and meat quality traits in a multi-

bioRxiv preprint doi: https://doi.org/10.1101/132696; this version posted June 8, 2017. The copyright holder for this preprint (which was not certified by peer review) is the author/funder. All rights reserved. No reuse allowed without permission.

breed sheep population using a HD SNP chip. BMC Genetics. 2017;18(1):7. doi: 10.1186/s12863-017-0476-8.

3. Hayes BJ, Lewin HA, Goddard ME. The future of livestock breeding: genomic selection for efficiency, reduced emissions intensity, and adaptation. Trends in Genetics. 2013;29(4):206-14. doi: doi.org/10.1016/j.tig.2012.11.009.

4. Daetwyler HD, Hickey JM, Henshall JM, Dominik S, Gredler B, van der Werf JHJ, et al. Accuracy of estimated genomic breeding values for wool and meat traits in a multi-breed sheep population. Animal Production Science. 2010;50(12):1004-10. doi: doi.org/10.1071/AN10096.

5. Wickramasinghe S, Cánovas A, Rincón G, Medrano JF. RNA-Sequencing: A tool to explore new frontiers in animal genetics. Livestock Science. 2014;166:206-16. doi: doi.org/10.1016/j.livsci.2014.06.015.

6. Freeman TC, Ivens A, Baillie JK, Beraldi D, Barnett MW, Dorward D, et al. A gene expression atlas of the domestic pig. BMC Biology. 2012;10(1):90. doi: 10.1186/1741-7007-10-90.

7. Harhay GP, Smith TP, Alexander LJ, Haudenschild CD, Keele JW, Matukumalli LK, et al. An atlas of bovine gene expression reveals novel distinctive tissue characteristics and evidence for improving genome annotation. Genome Biology. 2010;11(10):R102. doi: 10.1186/gb-2010-11-10-r102.

8. Su AI, Cooke MP, Ching KA, Hakak Y, Walker JR, Wiltshire T, et al. Large-scale analysis of the human and mouse transcriptomes. Proc Natl Acad Sci USA. 2002;99. doi: 10.1073/pnas.012025199.

9. Su AI, Wiltshire T, Batalov S, Lapp H, Ching KA, Block D, et al. A gene atlas of the mouse and human protein-encoding transcriptomes. Proc Natl Acad Sci USA. 2004;101. doi: 10.1073/pnas.0400782101.

bioRxiv preprint doi: https://doi.org/10.1101/132696; this version posted June 8, 2017. The copyright holder for this preprint (which was not certified by peer review) is the author/funder. All rights reserved. No reuse allowed without permission.

998 10. Mansour TA, Scott EY, Finno CJ, Bellone RR, Mienaltowski MJ, Penedo MC, et al.
999 Tissue resolved, gene structure refined equine transcriptome. BMC Genomics.
1000 2017;18(1):103. doi: 10.1186/s12864-016-3451-2.
1001 11. Andersson R, Gebhard C, Miguel-Escalada I, Hoof I, Bornholdt J, Boyd M, et al. An
1002 atlas of active enhancers across human cell types and tissues. Nature. 2014;507(7493):455-
1003 61. doi: doi.org/10.1038/nature12787.
1004 12. Lizio M, Harshbarger J, Shimoji H, Severin J, Kasukawa T, Sahin S, et al. Gateways
1005 to the FANTOM5 promoter level mammalian expression atlas. Genome Biology.
1006 2015;16(1):22. doi: 10.1186/s13059-014-0560-6.
1007 13. Forrest AR, Kawaji H, Rehli M, Baillie JK, De Hoon M, Haberle V, et al. A
1008 promoter-level mammalian expression atlas. Nature. 2014;507(7493):462-70. doi:
1009 doi.org/10.1038/nature13182.
1010 14. Birney E, Stamatoyannopoulos JA, Dutta A, Guigo R, Gingeras TR, Margulies EH, et
1011 al. Identification and analysis of functional elements in 1% of the human genome by the
1012 ENCODE pilot project. Nature. 2007;447. doi: 10.1038/nature05874.
1013 15. Melé M, Ferreira PG, Reverter F, DeLuca DS, Monlong J, Sammeth M, et al. The
1014 human transcriptome across tissues and individuals. Science. 2015;348(6235):660. doi: doi:
1015 10.1126/science.aaa0355.
1016 16. Bickhart DM, Rosen BD, Koren S, Sayre BL, Hastie AR, Chan S, et al. Single-
1017 molecule sequencing and chromatin conformation capture enable de novo reference assembly
1018 of the domestic goat genome. Nat Genet. 2017;49(4):643-50. doi: doi.org/10.1038/ng.3802.
1019 17. Worley KC. A golden goat genome. Nat Genet. 2017;49(4):485-6. doi:
1020 10.1038/ng.3824.

bioRxiv preprint doi: https://doi.org/10.1101/132696; this version posted June 8, 2017. The copyright holder for this preprint (which was not certified by peer review) is the author/funder. All rights reserved. No reuse allowed without permission.

1021 18. Jiang Y, Xie M, Chen W, Talbot R, Maddox JF, Faraut T, et al. The sheep genome
1022 illuminates biology of the rumen and lipid metabolism. Science. 2014;344(6188):1168. doi:
1023 doi: 10.1126/science.1252806.
1024 19. Krupp M, Marquardt JU, Sahin U, Galle PR, Castle J, Teufel A. RNA-Seq Atlas - A
1025 reference database for gene expression profiling in normal tissue by next generation
1026 sequencing. Bioinformatics. 2012;28. doi: 10.1093/bioinformatics/bts084.
1027 20. Oliver S. Proteomics: Guilt-by-association goes global. Nature. 2000;403(6770):601-
1028 3. doi: doi.org/10.1038/35001165.
1029 21. Xiang R, Oddy VH, Archibald AL, Vercoe PE, Dalrymple BP. Epithelial, metabolic
1030 and innate immunity transcriptomic signatures differentiating the rumen from other sheep
1031 and mammalian gastrointestinal tract tissues. PeerJ. 2016;4:e1762. doi: 10.7717/peerj.1762.
1032 22. Mabbott NA, Kenneth Baillie J, Hume DA, Freeman TC. Meta-analysis of lineage-
1033 specific gene expression signatures in mouse leukocyte populations. Immunobiology.
1034 2010;215. doi: 10.1016/j.imbio.2010.05.012.
1035 23. Mabbott NA, Kenneth Baillie J, Kobayashi A, Donaldson DS, Ohmori H, Yoon SO,
1036 et al. Expression of mesenchyme-specific gene signatures by follicular dendritic cells:
1037 insights from the meta-analysis of microarray data from multiple mouse cell populations.
1038 Immunology. 2011;133. doi: 10.1111/j.1365-2567.2011.03461.x.
1039 24. Clop A, Marcq F, Takeda H, Pirottin D, Tordoir X, Bibe B, et al. A mutation creating
1040 a potential illegitimate microRNA target site in the myostatin gene affects muscularity in
1041 sheep. Nat Genet. 2006;38(7):813-8. doi: doi.org/10.1038/ng1810.
1042 25. Blackface Sheep Breeders Association [1st March 2017]. Available from:
1043 http://www.scottish-blackface.co.uk/.
1044 26. Andersson L, Archibald AL, Bottema CD, Brauning R, Burgess SC, Burt DW, et al.
1045 Coordinated international action to accelerate genome-to-phenome with FAANG, the

bioRxiv preprint doi: https://doi.org/10.1101/132696; this version posted June 8, 2017. The copyright holder for this preprint (which was not certified by peer review) is the author/funder. All rights reserved. No reuse allowed without permission.

1046 Functional Annotation of Animal Genomes project. Genome Biology. 2015;16(1):57. doi:
1047 10.1186/s13059-015-0622-4.
1048 27. Tuggle CK, Giuffra E, White SN, Clarke L, Zhou H, Ross PJ, et al. GO-FAANG
1049 meeting: a Gathering On Functional Annotation of Animal Genomes. Animal Genetics.
1050 2016;47(5):528-33. doi: 10.1111/age.12466.
1051 28. Carninci P, Kasukawa T, Katayama S, Gough J, Frith MC, Maeda N, et al. The
1052 transcriptional landscape of the mammalian genome. Science. 2005;309. doi:
1053 10.1126/science.1112014.
1054 29. Bray NL, Pimentel H, Melsted P, Pachter L. Near-optimal probabilistic RNA-seq
1055 quantification. Nat Biotech. 2016;34(525–527). doi: doi.org/10.1038/nbt.3519.
1056 30. Robert C, Watson M. Errors in RNA-Seq quantification affect genes of relevance to
1057 human disease. Genome Biology. 2015;16:177. doi: 10.1186/s13059-015-0734-x.
1058 31. Bush SJ, McCulloch MEB, Summers KM, Hume DA, Clark EL. Integration of
1059 quantitated expression estimates from polyA-selected and rRNA-depleted RNA-seq libraries.
1060 BMC Bioinformatics. 2017;In Press.
1061 32. Guo S, Lim D, Dong Z, Saunders TL, Ma PX, Marcelo CL, et al. Dentin
1062 sialophosphoprotein: a regulatory protein for dental pulp stem cell identity and fate. Stem
1063 Cells Dev. 2014;23(23):2883-94. doi: 10.1089/scd.2014.0066.
1064 33. Wyatt K, Gao C, Tsai JY, Fariss RN, Ray S, Wistow G. A role for lengsin, a recruited
1065 enzyme, in terminal differentiation in the vertebrate lens. J Biol Chem. 2008;283(10):6607-
1066 15. doi: 10.1074/jbc.M709144200.
1067 34. Pruitt KD, Tatusova T, Maglott DR. NCBI Reference Sequence (RefSeq): a curated
1068 non-redundant sequence database of genomes, transcripts and proteins. Nucleic acids
1069 research. 2005;33(Database Issue):D501-D4. doi: 10.1093/nar/gki025.

bioRxiv preprint doi: https://doi.org/10.1101/132696; this version posted June 8, 2017. The copyright holder for this preprint (which was not certified by peer review) is the author/funder. All rights reserved. No reuse allowed without permission.

35. Freeman TC, Goldovsky L, Brosch M, van Dongen S, Maziere P, Grocock RJ, et al. Construction, visualisation, and clustering of transcription networks from microarray expression data. PLoS Computational Biology. 2007;3(10):2032-42. doi: 10.1371/journal.pcbi.0030206.

36. Theocharidis A, van Dongen S, Enright AJ, Freeman TC. Network visualization and analysis of gene expression data using BioLayout Express(3D). Nat Protoc. 2009;4(10):1535-50. Epub 2009/10/03. doi: 10.1038/nprot.2009.177.

37. Kajeka. Miru 見る 2016 [16th March 2017]. Available from: https://kajeka.com/miru/miru-about/.

38. van Dongen S, Abreu-Goodger C. Using MCL to extract clusters from networks. Methods Mol Biol. 2012;804:281-95. doi: 10.1007/978-1-61779-361-5_15.

39. Ashburner M, Ball CA, Blake JA, Botstein D, Butler H, Cherry JM, et al. Gene ontology: tool for the unification of biology. The Gene Ontology Consortium. Nat Genet. 2000;25. doi: 10.1038/75556.

40. Hume DA, Summers KM, Raza S, Baillie JK, Freeman TC. Functional clustering and lineage markers: insights into cellular differentiation and gene function from large-scale microarray studies of purified primary cell populations. Genomics. 2010;95. doi: 10.1016/j.ygeno.2010.03.002.

41. Stumvoll M, Meyer C, Perriello G, Kreider M, Welle S, Gerich J. Human kidney and liver gluconeogenesis: evidence for organ substrate selectivity. American Journal of Physiology - Endocrinology And Metabolism. 1998;274(5):E817.

42. Ayyar VS, Almon RR, DuBois DC, Sukumaran S, Qu J, Jusko WJ. Functional proteomic analysis of corticosteroid pharmacodynamics in rat liver: Relationship to hepatic stress, signaling, energy regulation, and drug metabolism. Journal of Proteomics. doi: doi.org/10.1016/j.jprot.2017.03.007.

bioRxiv preprint doi: https://doi.org/10.1101/132696; this version posted June 8, 2017. The copyright holder for this preprint (which was not certified by peer review) is the author/funder. All rights reserved. No reuse allowed without permission.

1095 43. FANTOM Consortium. ZENBU: a collaborative, omics data integration and
1096 interactive visualization system 2017 [27th March 2017]. Available from:
1097 http://fantom.gsc.riken.jp/zenbu/.
1098 44. Severin J, Lizio M, Harshbarger J, Kawaji H, Daub CO, Hayashizaki Y, et al.
1099 Interactive visualization and analysis of large-scale sequencing datasets using ZENBU. Nat
1100 Biotech. 2014;32(3):217-9. doi: doi.org/10.1038/nbt.2840.
1101 45. Basten SG, Giles RH. Functional aspects of primary cilia in signaling, cell cycle and
1102 tumorigenesis. Cilia. 2013;2(1):6. doi: 10.1186/2046-2530-2-6.
1103 46. Izawa I, Goto H, Kasahara K, Inagaki M. Current topics of functional links between
1104 primary cilia and cell cycle. Cilia. 2015;4(1):12. doi: 10.1186/s13630-015-0021-1.
1105 47. Jackson PK. Do cilia put brakes on the cell cycle? Nat Cell Biol. 2011;13. doi:
1106 10.1038/ncb0411-340.
1107 48. Doig TN, Hume DA, Theocharidis T, Goodlad JR, Gregory CD, Freeman TC.
1108 Coexpression analysis of large cancer datasets provides insight into the cellular phenotypes
1109 of the tumour microenvironment. BMC Genomics. 2013;14(1):469. doi: 10.1186/1471-2164-
1110 14-469.
1111 49. Calvo SE, Clauser KR, Mootha VK. MitoCarta2.0: an updated inventory of
1112 mammalian mitochondrial proteins. Nucleic Acids Research. 2016;44(Database
1113 issue):D1251-D7. doi: 10.1093/nar/gkv1003.
1114 50. Sharma S, Sud N, Wiseman DA, Carter AL, Kumar S, Hou Y, et al. Altered carnitine
1115 homeostasis is associated with decreased mitochondrial function and altered nitric oxide
1116 signaling in lambs with pulmonary hypertension. American Journal of Physiology - Lung
1117 Cellular and Molecular Physiology. 2008;294(1):L46. doi: 10.1152/ajplung.00247.2007.

bioRxiv preprint doi: https://doi.org/10.1101/132696; this version posted June 8, 2017. The copyright holder for this preprint (which was not certified by peer review) is the author/funder. All rights reserved. No reuse allowed without permission.

1118 51. McCommis KS, Finck BN. Mitochondrial pyruvate transport: a historical perspective
1119 and future research directions. The Biochemical Journal. 2015;466(3):443-54. doi:
1120 10.1042/BJ20141171.
1121 52. Xiang R, McNally J, Rowe S, Jonker A, Pinares-Patino CS, Oddy VH, et al. Gene
1122 network analysis identifies rumen epithelial cell proliferation, differentiation and metabolic
1123 pathways perturbed by diet and correlated with methane production. Scientific Reports.
1124 2016;6:39022. doi: doi.org/10.1038/srep39022.
1125 53. Hofmann RR. Evolutionary steps of ecophysiological adaptation and diversification
1126 of ruminants: a comparative view of their digestive system. Oecologia. 1989;78(4):443-57.
1127 doi: 10.1007/BF00378733.
1128 54. Rabbani I, Siegling-Vlitakis C, Noci B, Martens H. Evidence for NHE3-mediated Na
1129 transport in sheep and bovine forestomach. American Journal of Physiology - Regulatory,
1130 Integrative and Comparative Physiology. 2011;301(2):R313. doi:
1131 10.1152/ajpregu.00580.2010.
1132 55. Foster AM, Baliwag J, Chen CS, Guzman AM, Stoll SW, Gudjonsson JE, et al. IL-36
1133 Promotes Myeloid Cell Infiltration, Activation, and Inflammatory Activity in Skin. The
1134 Journal of Immunology. 2014;192(12):6053. doi: 10.4049/jimmunol.1301481.
1135 56. Perkins ND. Integrating cell-signalling pathways with NF-[kappa]B and IKK
1136 function. Nat Rev Mol Cell Biol. 2007;8(1):49-62. doi: 10.1038/nrm2083.
1137 57. Palmer C, Diehn M, Alizadeh AA, Brown PO. Cell-type specific gene expression
1138 profiles of leukocytes in human peripheral blood. BMC Genomics. 2006;7(1):115. doi:
1139 10.1186/1471-2164-7-115.
1140 58. Margraf S, Garner LI, Wilson TJ, Brown MH. A polymorphism in a phosphotyrosine
1141 signalling motif of CD229 (Ly9, SLAMF3) alters SH2 domain binding and T-cell activation.
1142 Immunology. 2015;146(3):392-400. doi: 10.1111/imm.12513.

bioRxiv preprint doi: https://doi.org/10.1101/132696; this version posted June 8, 2017. The copyright holder for this preprint (which was not certified by peer review) is the author/funder. All rights reserved. No reuse allowed without permission.

1143 59. Akira S, Takeda K. Toll-like receptor signalling. Nat Rev Immunol. 2004;4(7):499-
1144 511. doi: 10.1038/nri1391.
1145 60. Baillie JK, Arner E, Daub C, De Hoon M, Itoh M, Kawaji H, et al. Analysis of the
1146 human monocyte-derived macrophage transcriptome and response to lipopolysaccharide
1147 provides new insights into genetic aetiology of inflammatory bowel disease. PLoS Genetics.
1148 2017;13(3):e1006641. doi: 10.1371/journal.pgen.1006641.
1149 61. Pflanz S, Timans JC, Cheung J, Rosales R, Kanzler H, Gilbert J, et al. IL-27, a
1150 Heterodimeric Cytokine Composed of EBI3 and p28 Protein, Induces Proliferation of Naive
1151 CD4+ T Cells. Immunity. 2002;16(6):779-90. doi: doi.org/10.1016/S1074-7613(02)00324-2.
1152 62. Hume DA, Ross IL, Himes SR, Sasmono RT, Wells CA, Ravasi T. The mononuclear
1153 phagocyte system revisited. Journal of Leukocyte Biology. 2002;72(4):621-7.
1154 63. Moestrup SK, Moller HJ. CD163: a regulated hemoglobin scavenger receptor with a
1155 role in the anti-inflammatory response. Annals of Medicine. 2004;36(5):347-54.
1156 64. Bain CC, Mowat AM. Intestinal macrophages – specialised adaptation to a unique
1157 environment. European Journal of Immunology. 2011;41(9):2494-8. doi:
1158 10.1002/eji.201141714.
1159 65. Vogt L, Schmitz N, Kurrer MO, Bauer M, Hinton HI, Behnke S, et al. VSIG4, a B7
1160 family–related protein, is a negative regulator of T cell activation. Journal of Clinical
1161 Investigation. 2006;116(10):2817-26. doi: 10.1172/JCI25673.
1162 66. Luo L, Bokil NJ, Wall AA, Kapetanovic R, Lansdaal NM, Marceline F, et al. SCIMP
1163 is a transmembrane non-TIR TLR adaptor that promotes proinflammatory cytokine
1164 production from macrophages. Nature Communications. 2017;8:14133. doi:
1165 10.1038/ncomms14133.
1166 67. Bonifer C, Hume DA. The transcriptional regulation of the Colony-Stimulating Factor
1167 1 Receptor (csf1r) gene during hematopoiesis Frontiers in Bioscience. 2008;(13):549-60.

bioRxiv preprint doi: https://doi.org/10.1101/132696; this version posted June 8, 2017. The copyright holder for this preprint (which was not certified by peer review) is the author/funder. All rights reserved. No reuse allowed without permission.

1168 68. Hume DA, Yue X, Ross IL, Favot P, Lichanska A, Ostrowski MC. Regulation of
1169 CSF-1 receptor expression. Molecular Reproduction and Development. 1997;46(1):46-53.
1170 doi: 10.1002/(SICI)1098-2795(199701)46:1<46::AID-MRD8>3.0.CO;2-R.
1171 69. Uhlén M, Fagerberg L, Hallström BM, Lindskog C, Oksvold P, Mardinoglu A, et al.
1172 Tissue-based map of the human proteome. Science. 2015;347(6220). doi:
1173 10.1126/science.1260419.
1174 70. Wu C, Jin X, Tsueng G, Afrasiabi C, Su AI. BioGPS: building your own mash-up of
1175 gene annotations and expression profiles. Nucleic Acids Research. 2016;44(D1):D313-D6.
1176 doi: 10.1093/nar/gkv1104.
1177 71. Djureinovic D, Fagerberg L, Hallström B, Danielsson A, Lindskog C, Uhlén M, et al.
1178 The human testis-specific proteome defined by transcriptomics and antibody-based profiling.
1179 MHR: Basic science of reproductive medicine. 2014;20(6):476-88. doi:
1180 10.1093/molehr/gau018.
1181 72. Yu NY-L, Hallström BM, Fagerberg L, Ponten F, Kawaji H, Carninci P, et al.
1182 Complementing tissue characterization by integrating transcriptome profiling from the
1183 Human Protein Atlas and from the FANTOM5 consortium. Nucleic Acids Research.
1184 2015;43(14):6787-98. doi: 10.1093/nar/gkv608.
1185 73. Baillet A, Le Bouffant R, Volff JN, Luangpraseuth A, Poumerol E, Thépot D, et al.
1186 TOPAZ1, a Novel Germ Cell-Specific Expressed Gene Conserved during Evolution across
1187 Vertebrates. PLoS ONE. 2011;6(11):e26950. doi: 10.1371/journal.pone.0026950.
1188 74. Olesen C, Larsen NJ, Byskov AG, Harboe TL, Tommerup N. Human FATE is a
1189 novel X-linked gene expressed in fetal and adult testis. Molecular and Cellular
1190 Endocrinology. 2001;184(1–2):25-32. doi: doi.org/10.1016/S0303-7207(01)00666-9.

bioRxiv preprint doi: https://doi.org/10.1101/132696; this version posted June 8, 2017. The copyright holder for this preprint (which was not certified by peer review) is the author/funder. All rights reserved. No reuse allowed without permission.

1191 75. Osaki E, Nishina Y, Inazawa J, Copeland NG, Gilbert DJ, Jenkins NA, et al.
1192 Identification of a novel Sry-related gene and its germ cell-specific expression. Nucleic Acids
1193 Research. 1999;27(12):2503-10.
1194 76. Calloni R, Cordero EAA, Henriques JAP, Bonatto D. Reviewing and Updating the
1195 Major Molecular Markers for Stem Cells. Stem Cells and Development. 2013;22(9):1455-76.
1196 doi: 10.1089/scd.2012.0637.
1197 77. Kehler J, Tolkunova E, Koschorz B, Pesce M, Gentile L, Boiani M, et al. Oct4 is
1198 required for primordial germ cell survival. EMBO reports. 2004;5(11):1078-83. doi:
1199 10.1038/sj.embor.7400279.
1200 78. Juengel JL, Bodensteiner KJ, Heath DA, Hudson NL, Moeller CL, Smith P, et al.
1201 Physiology of GDF9 and BMP15 signalling molecules. Animal Reproduction Science.
1202 2004;82–83:447-60. doi: doi.org/10.1016/j.anireprosci.2004.04.021.
1203 79. McNatty KP, Juengel JL, Wilson T, Galloway SM, Davis GH. Genetic mutations
1204 influencing ovulation rate in sheep. Reproduction, Fertility and Development.
1205 2002;13(8):549-55.
1206 80. Davis GH. Major genes affecting ovulation rate in sheep. Genetics Selection
1207 Evolution : GSE. 2005;37(Suppl 1):S11-S23. doi: 10.1186/1297-9686-37-S1-S11.
1208 81. Palomera CL, Morales RAA. Genes with major effect on fertility in sheep. Revista
1209 Mexicana de Ciencias Pecuarias. 2014;5(1):107-30.
1210 82. Davis GH. Fecundity genes in sheep. Animal Reproduction Science. 2004;82:247-53.
1211 doi: http://dx.doi.org/10.1016/j.anireprosci.2004.04.001.
1212 83. Imahara SD, Jelacic S, Junker CE, O'Keefe GE. The influence of gender on human
1213 innate immunity. Surgery. 2005;138(2):275-82. doi: doi.org/10.1016/j.surg.2005.03.020.
1214 84. Marriott I, Huet-Hudson YM. Sexual dimorphism in innate immune responses to
1215 infectious organisms. Immunologic Research. 2006;34(3):177-92. doi: 10.1385/IR:34:3:177.

bioRxiv preprint doi: https://doi.org/10.1101/132696; this version posted June 8, 2017. The copyright holder for this preprint (which was not certified by peer review) is the author/funder. All rights reserved. No reuse allowed without permission.

85. Everhardt Queen A, Moerdyk-Schauwecker M, McKee LM, Leamy LJ, Huet YM. Differential Expression of Inflammatory Cytokines and Stress Genes in Male and Female Mice in Response to a Lipopolysaccharide Challenge. PLoS ONE. 2016;11(4):e0152289. doi: 10.1371/journal.pone.0152289.

86. Lamason R, Zhao P, Rawat R, Davis A, Hall JC, Chae JJ, et al. Sexual dimorphism in immune response genes as a function of puberty. BMC Immunology. 2006;7(1):2. doi: 10.1186/1471-2172-7-2.

87. Forde N, Maillo V, O'Gaora P, Simintiras CA, Sturmey RG, Ealy AD, et al. Sexually Dimorphic Gene Expression in Bovine Conceptuses at the Initiation of Implantation. Biology of Reproduction. 2016;95(4):92, 1-8-, 1-8. doi: 10.1095/biolreprod.116.139857.

88. Bermejo-Alvarez P, Rizos D, Rath D, Lonergan P, Gutierrez-Adan A. Sex determines the expression level of one third of the actively expressed genes in bovine blastocysts. Proc Natl Acad Sci USA. 2010;107. doi: 10.1073/pnas.0913843107.

89. Mentzel CMJ, Anthon C, Jacobsen MJ, Karlskov-Mortensen P, Bruun CS, Jørgensen CB, et al. Gender and Obesity Specific MicroRNA Expression in Adipose Tissue from Lean and Obese Pigs. PLoS ONE. 2015;10(7):e0131650. doi: 10.1371/journal.pone.0131650.

90. Zhang J, Zhou C, Ma J, Chen L, Jiang A, Zhu L, et al. Breed, sex and anatomical location-specific gene expression profiling of the porcine skeletal muscles. BMC Genetics. 2013;14(1):53. doi: 10.1186/1471-2156-14-53.

91. Wood Shona H, Christian Helen C, Miedzinska K, Saer Ben RC, Johnson M, Paton B, et al. Binary Switching of Calendar Cells in the Pituitary Defines the Phase of the Circannual Cycle in Mammals. Current Biology. 2015;25(20):2651-62. doi: doi.org/10.1016/j.cub.2015.09.014.

bioRxiv preprint doi: https://doi.org/10.1101/132696; this version posted June 8, 2017. The copyright holder for this preprint (which was not certified by peer review) is the author/funder. All rights reserved. No reuse allowed without permission.

1239 92. Bjelobaba I, Janjic MM, Kucka M, Stojilkovic SS. Cell Type-Specific Sexual
1240 Dimorphism in Rat Pituitary Gene Expression During Maturation. Biology of Reproduction.
1241 2015;93(1):21. doi: 10.1095/biolreprod.115.129320.
1242 93. Oidovsambuu O, Nyamsuren G, Liu S, Göring W, Engel W, Adham IM. Adhesion
1243 Protein VSIG1 Is Required for the Proper Differentiation of Glandular Gastric Epithelia.
1244 PLoS ONE. 2011;6(10):e25908. doi: 10.1371/journal.pone.0025908.
1245 94. Ellegren H, Parsch J. The evolution of sex-biased genes and sex-biased gene
1246 expression. Nat Rev Genet. 2007;8(9):689-98. doi: 10.1038/nrg2167.
1247 95. Gillespie JR, Flanders F. Modern Livestock & Poultry Production. 8th Edition ed:
1248 Delmar; 2009.
1249 96. Zonabend König E, Ojango JMK, Audho J, Mirkena T, Strandberg E, Okeyo AM, et
1250 al. Live weight, conformation, carcass traits and economic values of ram lambs of Red
1251 Maasai and Dorper sheep and their crosses. Tropical Animal Health and Production.
1252 2017;49(1):121-9. doi: 10.1007/s11250-016-1168-5.
1253 97. Zonabend König E, Strandberg E, Ojango JMK, Mirkena T, Okeyo AM, Philipsson J.
1254 Purebreeding of Red Maasai and crossbreeding with Dorper sheep in different environments
1255 in Kenya. Journal of Animal Breeding and Genetics. 2017:n/a-n/a. doi: 10.1111/jbg.12260.
1256 98. Rashid MM, Runci A, Polletta L, Carnevale I, Morgante E, Foglio E, et al. Muscle
1257 LIM protein/CSRP3: a mechanosensor with a role in autophagy. Cell Death Discovery.
1258 2015;1:15014. doi: doi.org/10.1038/cddiscovery.2015.14.
1259 99. Jan AT, Lee EJ, Choi I. Fibromodulin: A regulatory molecule maintaining cellular
1260 architecture for normal cellular function. Int J Biochem Cell Biol. 2016;80:66-70. Epub
1261 2016/10/04. doi: 10.1016/j.biocel.2016.09.023.

bioRxiv preprint doi: https://doi.org/10.1101/132696; this version posted June 8, 2017. The copyright holder for this preprint (which was not certified by peer review) is the author/funder. All rights reserved. No reuse allowed without permission.

100. Funderburgh JL, Mann MM, Funderburgh ML. Keratocyte Phenotype Mediates Proteoglycan Structure: A Role for Fibroblasts in Corneal Fibrosis. The Journal of Biological Chemistry. 2003;278(46):45629-37. doi: 10.1074/jbc.M303292200.

101. Hadler-Olsen E, Solli AI, Hafstad A, Winberg JO, Uhlin-Hansen L. Intracellular MMP-2 activity in skeletal muscle is associated with type II fibers. J Cell Physiol. 2015;230(1):160-9. Epub 2014/06/07. doi: 10.1002/jcp.24694.

102. Beard NA, Laver DR, Dulhunty AF. Calsequestrin and the calcium release channel of skeletal and cardiac muscle. Prog Biophys Mol Biol. 2004;85(1):33-69. Epub 2004/03/31. doi: 10.1016/j.pbiomolbio.2003.07.001.

103. Tellam RL, Cockett NE, Vuocolo T, Bidwell CA. Genes Contributing to Genetic Variation of Muscling in Sheep. Frontiers in Genetics. 2012;3:164. doi: 10.3389/fgene.2012.00164.

104. Miar Y, Salehi A, Kolbehdari D, Aleyasin SA. Application of myostatin in sheep breeding programs: A review. Molecular Biology Research Communications. 2014;3(1):33-43.

105. Cassar-Malek I, Passelaigue F, Bernard C, Léger J, Hocquette J-F. Target genes of myostatin loss-of-function in muscles of late bovine fetuses. BMC Genomics. 2007;8:63. doi: DOI: 10.1186/1471-2164-8-63.

106. Wang M, Yu H, Kim YS, Bidwell CA, Kuang S. Myostatin facilitates slow and inhibits fast myosin heavy chain expression during myogenic differentiation. Biochemical and Biophysical Research Communications. 2012;426(1):83-8. doi: doi.org/10.1016/j.bbrc.2012.08.040.

107. Allen DL, Loh AS. Posttranscriptional mechanisms involving microRNA-27a and b contribute to fast-specific and glucocorticoid-mediated myostatin expression in skeletal

bioRxiv preprint doi: https://doi.org/10.1101/132696; this version posted June 8, 2017. The copyright holder for this preprint (which was not certified by peer review) is the author/funder. All rights reserved. No reuse allowed without permission.

muscle. American Journal of Physiology - Cell Physiology. 2011;300(1):C124-C37. doi: 10.1152/ajpcell.00142.2010.

108. Mosca B, Eckhardt J, Bergamelli L, Treves S, Bongianino R, De Negri M, et al. Role of the JP45-Calsequestrin Complex on Calcium Entry in Slow Twitch Skeletal Muscles. Journal of Biological Chemistry. 2016;291(28):14555-65. doi: 10.1074/jbc.M115.709071.

109. Moran CM, Garriock RJ, Miller MK, Heimark RL, Mudry RE, Gregorio CC, et al. Expression of the fast twitch troponin complex, fTnT, fTnI and fTnC, in vascular smooth muscle. Cell motility and the cytoskeleton. 2008;65(8):652-61. doi: 10.1002/cm.20291.

110. Odermatt A, Becker S, Khanna VK, Kurzydlowski K, Leisner E, Pette D, et al. Sarcolipin Regulates the Activity of SERCA1, the Fast-twitch Skeletal Muscle Sarcoplasmic Reticulum Ca2+-ATPase. Journal of Biological Chemistry. 1998;273(20):12360-9. doi: 10.1074/jbc.273.20.12360.

111. Joo ST, Kim GD, Hwang YH, Ryu YC. Control of fresh meat quality through manipulation of muscle fiber characteristics. Meat Science. 2013;95(4):828-36. doi: doi.org/10.1016/j.meatsci.2013.04.044.

112. Goel M, Sienkiewicz AE, Picciani R, Wang J, Lee RK, Bhattacharya SK. Cochlin, Intraocular Pressure Regulation and Mechanosensing. PLoS ONE. 2012;7(4):e34309. doi: 10.1371/journal.pone.0034309.

113. Seidenbecher CI, Smalla KH, Fischer N, Gundelfinger ED, Kreutz MR. Brevican isoforms associate with neural membranes. J Neurochem. 2002;83(3):738-46.

114. Yamaguchi Y. Brevican: a major proteoglycan in adult brain. Perspect Dev Neurobiol. 1996;3(4):307-17.

115. Holz A, Schwab ME. Developmental expression of the myelin gene MOBP in the rat nervous system. J Neurocytol. 1997;26(7):467-77.

bioRxiv preprint doi: https://doi.org/10.1101/132696; this version posted June 8, 2017. The copyright holder for this preprint (which was not certified by peer review) is the author/funder. All rights reserved. No reuse allowed without permission.

116. Yoshikawa F, Sato Y, Tohyama K, Akagi T, Hashikawa T, Nagakura-Takagi Y, et al. Opalin, a Transmembrane Sialylglycoprotein Located in the Central Nervous System Myelin Paranodal Loop Membrane. The Journal of Biological Chemistry. 2008;283(30):20830-40. doi: 10.1074/jbc.M801314200.

117. Boggs JM. Myelin basic protein: a multifunctional protein. Cellular and Molecular Life Sciences. 2006;63(17):1945-61. doi: 10.1007/s00018-006-6094-7.

118. Dwyer CM, Lawrence AB, Brown HE, Simm G. Effect of ewe and lamb genotype on gestation length, lambing ease and neonatal behaviour of lambs. Reprod Fertil Dev 1996;8(8):1123-9.

119. McCloskey E, McAdam JH. Grazing patterns and habitat selection of the Scottish Blackface compared with a crossbred, using GPS Satellite telemetry collars. Advances in Animal Biosciences. 2010;1(1):171. doi: 10.1017/S2040470010003146.

120. Wu C, MacLeod I, Su AI. BioGPS and MyGene.info: organizing online, gene-centric information. Nucleic Acids Research. 2013;41(D1):D561-D5. doi: 10.1093/nar/gks1114.

121. Wu C, Orozco C, Boyer J, Leglise M, Goodale J, Batalov S, et al. BioGPS: an extensible and customizable portal for querying and organizing gene annotation resources. Genome Biology. 2009;10(11):R130. doi: 10.1186/gb-2009-10-11-r130.

122. Kim D, Langmead B, Salzberg SL. HISAT: a fast spliced aligner with low memory requirements. Nat Meth. 2015;12(4):357-60. doi: doi.org/10.1038/nmeth.3317.

123. Pertea M, Pertea GM, Antonescu CM, Chang T-C, Mendell JT, Salzberg SL. StringTie enables improved reconstruction of a transcriptome from RNA-seq reads. Nat Biotech. 2015;33(3):290-5. doi: doi.org/10.1038/nbt.3122.

124. Miao X, Luo Q, Qin X. Genome-wide analysis reveals the differential regulations of mRNAs and miRNAs in Dorset and Small Tail Han sheep muscles. Gene. 2015;562(2):188-96. doi: doi.org/10.1016/j.gene.2015.02.070.

bioRxiv preprint doi: https://doi.org/10.1101/132696; this version posted June 8, 2017. The copyright holder for this preprint (which was not certified by peer review) is the author/funder. All rights reserved. No reuse allowed without permission.

125. Suárez-Vega A, Gutiérrez-Gil B, Klopp C, Tosser-Klopp G, Arranz JJ. Variant discovery in the sheep milk transcriptome using RNA sequencing. BMC Genomics. 2017;18(1):170. doi: 10.1186/s12864-017-3581-1.

126. Sun L, Bai M, Xiang L, Zhang G, Ma W, Jiang H. Comparative transcriptome profiling of longissimus muscle tissues from Qianhua Mutton Merino and Small Tail Han sheep. Scientific Reports. 2016;6:33586. doi: doi.org/10.1038/srep33586.

127. Peñagaricano F, Valente BD, Steibel JP, Bates RO, Ernst CW, Khatib H, et al. Searching for causal networks involving latent variables in complex traits: Application to growth, carcass, and meat quality traits in pigs. Journal of Animal Science. 2015;93(10):4617-23. doi: 10.2527/jas.2015-9213.

128. Van Laere A-S, Nguyen M, Braunschweig M, Nezer C, Collette C, Moreau L, et al. A regulatory mutation in IGF2 causes a major QTL effect on muscle growth in the pig. Nature. 2003;425(6960):832-6. doi: doi.org/10.1038/nature02064.

129. Banos G, Bramis G, Bush SJ, Clark EL, McCulloch MEB, Smith J, et al. The genomic architecture of mastitis resistance in dairy sheep. 2017;Under Review.

130. Suárez-Vega A, Gutiérrez-Gil B, Klopp C, Tosser-Klopp G, Arranz J-J. Comprehensive RNA-Seq profiling to evaluate lactating sheep mammary gland transcriptome. Scientific Data. 2016;3:160051. doi: doi.org/10.1038/sdata.2016.51.

131. Kapetanovic R, Fairbairn L, Beraldi D, Sester DP, Archibald AL, Tuggle CK, et al. Pig bone marrow-derived macrophages resemble human macrophages in their response to bacterial lipopolysaccharide. J Immunol. 2012;188. doi: 10.4049/jimmunol.1102649.

132. Fairbairn L, Kapetanovic R, Beraldi D, Sester DP, Tuggle CK, Archibald AL, et al. Comparative Analysis of Monocyte Subsets in the Pig. The Journal of Immunology. 2013;190(12):6389-96. doi: 10.4049/jimmunol.1300365.

bioRxiv preprint doi: https://doi.org/10.1101/132696; this version posted June 8, 2017. The copyright holder for this preprint (which was not certified by peer review) is the author/funder. All rights reserved. No reuse allowed without permission.

133. Montgomery GW, Sise JA. Extraction of DNA from sheep white blood cells. New Zealand Journal of Agricultural Research. 1990;33(3):437-41. doi: 10.1080/00288233.1990.10428440.

134. Pervouchine DD, Djebali S, Breschi A, Davis CA, Barja PP, Dobin A, et al. Enhanced transcriptome maps from multiple mouse tissues reveal evolutionary constraint in gene expression. Nat Commun. 2015;6. doi: 10.1038/ncomms6903.

135. Chitwood J, Rincon G, Kaiser G, Medrano J, Ross P. RNA-seq analysis of single bovine blastocysts. BMC Genomics. 2013;14(1):350. doi: 10.1186/1471-2164-14-350.

136. Martherus RS, Sluiter W, Timmer ED, VanHerle SJ, Smeets HJ, Ayoubi TA. Functional annotation of heart enriched mitochondrial genes GBAS and CHCHD10 through guilt by association. Biochem Biophys Res Commun. 2010;402. doi: 10.1016/j.bbrc.2010.09.109.

137. Alexa A, Rahnenfuhrer J. topGO: Enrichment analysis for Gene Ontology 2010. Available from: http://www.bioconductor.org/packages/release/bioc/html/topGO.html.

138. Fagerberg L, Hallström BM, Oksvold P, Kampf C, Djureinovic D, Odeberg J, et al. Analysis of the Human Tissue-specific Expression by Genome-wide Integration of Transcriptomics and Antibody-based Proteomics. Molecular & Cellular Proteomics. 2014;13(2):397-406. doi: 10.1074/mcp.M113.035600.

139. Lein ES, Hawrylycz MJ, Ao N, Ayres M, Bensinger A, Bernard A, et al. Genome-wide atlas of gene expression in the adult mouse brain. Nature. 2007;445(7124):168-76. doi: doi.org/10.1038/nature05453.

140. Siddiqui AS, Khattra J, Delaney AD, Zhao Y, Astell C, Asano J, et al. A mouse atlas of gene expression: Large-scale digital gene-expression profiles from precisely defined developing C57BL/6J mouse tissues and cells. Proc Natl Acad Sci USA. 2005;102(51):18485-90. doi: 10.1073/pnas.0509455102.

bioRxiv preprint doi: https://doi.org/10.1101/132696; this version posted June 8, 2017. The copyright holder for this preprint (which was not certified by peer review) is the author/funder. All rights reserved. No reuse allowed without permission.

141. Kumar S, Stecher G, Tamura K. MEGA7: Molecular Evolutionary Genetics Analysis Version 7.0 for Bigger Datasets. Molecular Biology and Evolution. 2016;33(7):1870-4. doi: 10.1093/molbev/msw054.

142. Rambaut A. FigTree v1.4.0 2016 [16th March 2017]. v1.4.3:[Available from: http://tree.bio.ed.ac.uk/software/figtree/.

Fig 1: Hierarchical clustering of the samples included in the sheep gene expression atlas dataset. Samples of each tissue and cell type from each breed and developmental stage were averaged across individuals for ease of visualisation. The tree was constructed from the Euclidean distances between expression vectors using MEGA v7.0.14 [141] with the neighbour-joining method and edited in the graphical viewer FigTree v1.4.3 [142]. Clustering is biologically meaningful and highlights the lack of any significant effect of library type post-correction. Samples are coloured by organ system.

Fig 2: Network visualisation and clustering of the sheep gene expression atlas. A three-dimensional visualisation of a Pearson correlation gene-to-gene graph of expression levels derived from RNA-Seq data from analysis of sheep tissues and cells. Each node (sphere) in the graph represents a gene and the edges (lines) correspond to correlations between individual measurements above the defined threshold. The graph is comprised of 15,192 nodes (genes) and 811,213 edges (correlations $\geq$0.75). Co-expressed genes form highly connected complex clusters within the graph. Genes were assigned to groups according to their level of co-expression using the MCL algorithm.

Fig 3: Collapsed node visualisation of the sheep gene expression atlas dataset in two-dimensions to illustrate the relative proportion of genes in each cluster. Includes 3104

bioRxiv preprint doi: https://doi.org/10.1101/132696; this version posted June 8, 2017. The copyright holder for this preprint (which was not certified by peer review) is the author/funder. All rights reserved. No reuse allowed without permission.

nodes and 138,407 edges with a Pearson correlation value of *r*=0.75 and an MCL inflation (MCLi) value of 2.2. Nodes are coloured by tissue/cell type or for broader classes organ system. The largest clusters are numbered from 1 to 30 (see Table 3 for functional annotation). The largest clusters are dominated by either house-keeping genes (1 & 4) or genes associated with transcriptionally rich tissues or cell types, such as brain (2), testes (3) and macrophages (5).

Fig 4: **Interrogation of the underlying expression profiles allows regions of the graph to be associated with specific tissues or cell types. A** A three-dimensional visualisation of a Pearson correlation gene to gene network graph (*r*=0.75, MCLi=2.2). Samples of each tissue and cell type from each breed and developmental stage are averaged across individuals for ease of visualisation. Histograms of the averaged expression profile (averaged across individuals for each tissue and cell type for ease of visualisation) of genes in selected clusters are given on the right: **B (i)** profile of cluster 5 genes whose expression is highest in macrophages; **(ii)** profile of cluster 7 genes whose expression is highest in fetal ovary and testes; **(iii)** or a broader expression pattern associated with a cellular process e.g. oxidative phosphorylation (cluster 15). Note that there may be a degree of variation in the expression pattern of individual genes within a cluster which is masked when average profiles are displayed.

Fig 5: Upregulation of genes in the crossbred BFxT relative to the purebred Texel. A A Texel sire was crossed with Scottish Blackface dam to create the F1 Texel x Scottish Blackface individuals. **B** The top 20 genes showing the greatest up-regulation (as absolute fold change) between the crossbred BFxT and purebred Texel individuals. Genes associated with the function of skeletal muscle and connective tissue are indicated.

bioRxiv preprint doi: https://doi.org/10.1101/132696; this version posted June 8, 2017. The copyright holder for this preprint (which was not certified by peer review) is the author/funder. All rights reserved. No reuse allowed without permission.

Fig 6: Screenshot of the representation of the profile of the sheep *GDF-8* (*MSTN*) gene within the BioGPS online portal. All data from the BFxT sheep gene expression atlas dataset are available through the BioGPS database (http://biogps.org/dataset/BDS_00015/sheep-atlas/). This provides a searchable database of genes, with expression profiles across tissues and cells for each gene displayed as histograms via the following link, http://biogps.org/sheepatlas/. Samples are coloured according to organ system, for example, Immune, GI Tract etc. The BioGPS platform supports searching for genes with a similar profile, allows access to the raw data, and links to external resources. It also provides the potential for comparative analysis across species, for example with the expression profiles for pig.

Supplemental Material

S1 Fig: Principal component analysis with all samples plotted in two dimensions using their projections onto the first two principal components. For each sample, each gene's expression level is taken as the mean TPM across all replicates, before (**A**) and after (**B**) any batch effect correction. Samples are coloured by organ system. Ellipses indicate confidence intervals of 95%. The shape of each point indicates each sample's library type: mRNA-seq (circle) or total RNA-seq (triangle). Blastocyst samples are excluded for clarity as they are generated using a different experimental protocol. Before correction, points can be partitioned by shape (to the left and right of sub-Fig A), suggesting a batch effect – variation introduced by library type confounds variation by tissue type. After correction (sub-Fig B), there is no notable axis of variation that partitions points by shape – consequently,

bioRxiv preprint doi: https://doi.org/10.1101/132696; this version posted June 8, 2017. The copyright holder for this preprint (which was not certified by peer review) is the author/funder. All rights reserved. No reuse allowed without permission.

variation introduced by library type (a batch effect) does not confound variation by tissue type (which is biologically meaningful).

S2 Fig: Sample-to-sample network graph analysis was used to validate the samples included in the sheep gene expression atlas dataset. Each node represents a sample and each edge its connectivity to other samples in the dataset. A correlation of r=0.75 split the graph into 10 different clusters. The largest cluster (cluster 1) included the majority of samples ('mixed tissues'), most of which were transcriptionally similar, while the remainder of the clusters comprised samples with distinctive transcriptional signatures such as macrophages (3) and abomasum. Spurious samples were easily identified if they were present in a cluster comprised of samples from a different tissue or cell type. Pearson Correlation r=0.75, MCLi = 2.2, nodes = 481 and edges = 23,903.

S1 Methods: Additional Methods

S1 Dataset: Gene Expression Level Atlas as transcripts per million (unaveraged)

S2 Dataset: Gene Expression Level Atlas as transcripts per million (averaged across biological replicates for each developmental stage)

S3 Dataset: Sex-biased Expression Atlas (based on expression estimates from 3 adult male and 3 adult female BFxT sheep)

S1 Table: Overview of animals used to generate the sheep atlas tissue subsets.

S2 Table: Details of library type and tissue/cell samples used in each subset of samples.

S3 Table: Number of reads, and number of aligned reads, per sample.

S4 Table: Genes undetected (TPM < 1) in every tissue/cell line of the expression atlas.

bioRxiv preprint doi: https://doi.org/10.1101/132696; this version posted June 8, 2017. The copyright holder for this preprint (which was not certified by peer review) is the author/funder. All rights reserved. No reuse allowed without permission.

S5 Table: Quality categories for automated gene annotations.

S6 Table: Proportion of unannotated protein-coding genes assigned probable gene names.

S7 Table: Source of ruminant proteome data.

S8 Table: Candidate gene names for unannotated Oar v3.1 protein-coding genes: shortlist.

S9 Table: Candidate gene names for unannotated Oar v3.1 protein-coding genes: longlist.

S10 Table: Candidate gene descriptions for all unannotated Oar v3.1. protein-coding genes (potentially informative in the absence of a gene name).

S11 Table: Genes within each co-expression cluster.

S12 Table: GO term enrichment for co-expression clusters 1 to 50.

S13 Table: Manual annotation of cluster 15 (genes involved in oxidative phosphorylation).

S14 Table: Manual annotation of unannotated genes in cluster 12 (genes with a T-cell signature).

S15 Table: Manual annotation of unannotated genes in cluster 5 (genes with an alveolar macrophage signature).

S16 Table: Genes with five-fold sex-biased expression in at least one BFxT tissue.

S17 Table: GO term enrichment for the set of genes with five-fold sex-biased expression in at least one BFxT tissue.

S18 Table: Fold changes in expression level between BFxT and Texel sheep.

S19 Table: GO term enrichment for the set of genes differentially expressed between BFxT and Texel sheep.

S20 Table: Number of genes with detectable expression, per tissue.

S21 Table: Coding potential of putative novel CDS.

S22 Table: Number of genes with detectable expression, per gene type.

S23 Table: Proportion of Oar v3.1 gene, exon and transcript models in the StringTie assembly.

bioRxiv preprint doi: https://doi.org/10.1101/132696; this version posted June 8, 2017. The copyright holder for this preprint (which was not certified by peer review) is the author/funder. All rights reserved. No reuse allowed without permission.

1508 **S24 Table:** Novel transcript models in the StringTie assembly.

1509 **S25 Table:** Details of the additional RNA-Seq libraries included from Texel sheep [18].

1510

1511

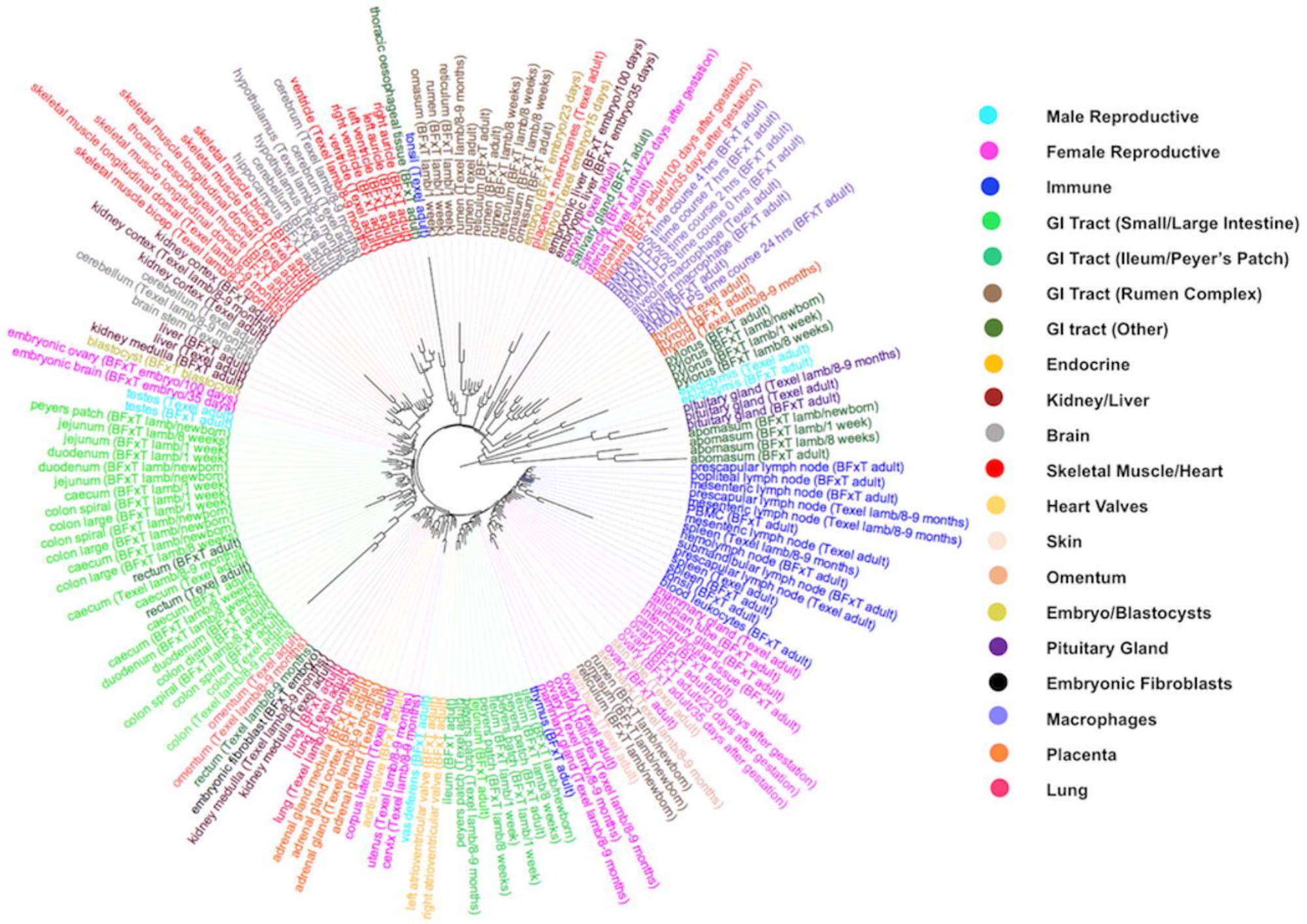
Male Reproductive
Female Reproductive
Immune
GI Tract (Small/Large Intestine)
GI Tract (Ileum/Peyer's Patch)
GI Tract (Rumen Complex)
GI tract (Other)
Endocrine
Kidney/Liver
Brain
Skeletal Muscle/Heart
Heart Valves
Skin
Omentum
Embryo/Blastocysts
Pituitary Gland
Embryonic Fibroblasts
Macrophages
Placenta
Lung

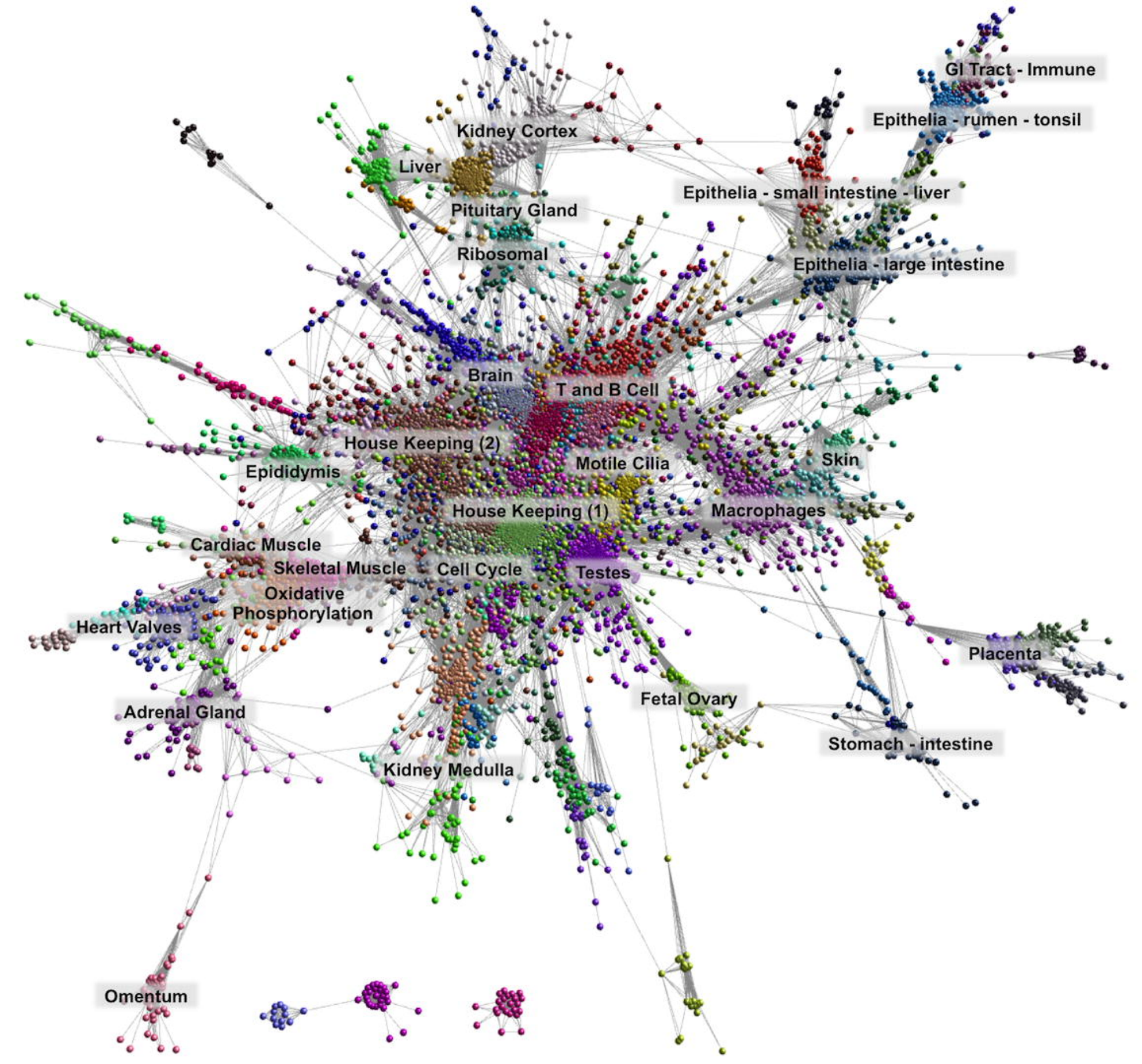
GI Tract - Immune
Epithelia - rumen - tonsil
Kidney Cortex
Liver
Epithelia - small intestine - liver
Pituitary Gland
Ribosomal
Epithelia - large intestine
Brain
T and B Cell
House Keeping (2)
Epididymis
Motile Cilia
Skin
House Keeping (1)
Macrophages
Cardiac Muscle
Skeletal Muscle
Cell Cycle
Testes
Oxidative
Phosphorylation
Heart Valves
Placenta
Fetal Ovary
Adrenal Gland
Stomach - intestine
Kidney Medulla
Omentum

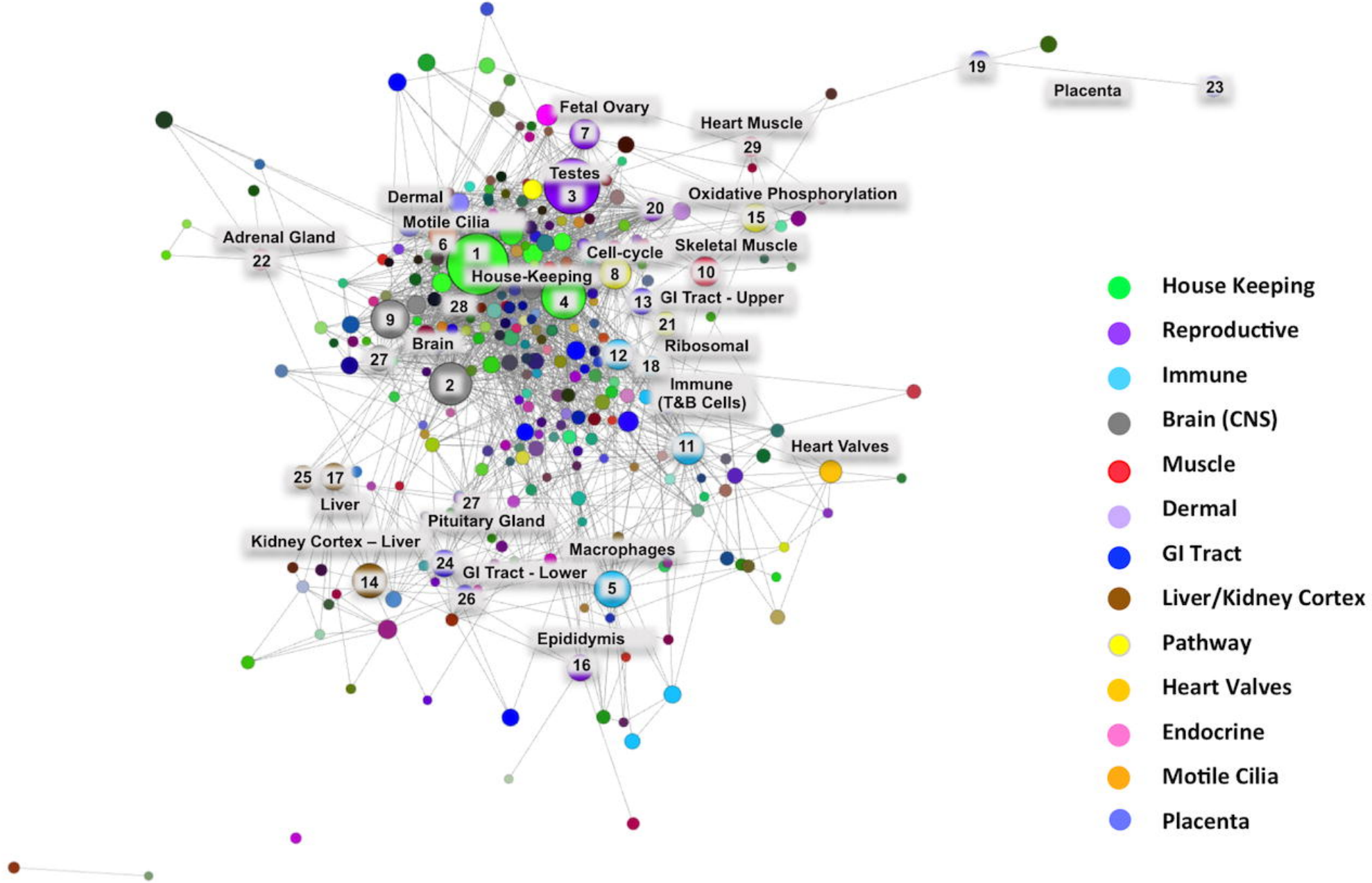
19
Placenta
23
Fetal Ovary
7
Heart Muscle
29
Testes
3
Dermal
Oxidative Phosphorylation
20
15
Motile Cilia
Adrenal Gland
6
1
Cell-cycle
Skeletal Muscle
22
House-Keeping
8
10
4
13
GI Tract - Upper
28
9
21
Brain
Ribosomal
27
12
18
2
Immune
(T&B Cells)
11
Heart Valves
25
17
Liver
27
Pituitary Gland
Kidney Cortex – Liver
Macrophages
24
GI Tract - Lower
14
5
26
Epididymis
16
House Keeping
Reproductive
Immune
Brain (CNS)
Muscle
Dermal
GI Tract
Liver/Kidney Cortex
Pathway
Heart Valves
Endocrine
Motile Cilia
Placenta

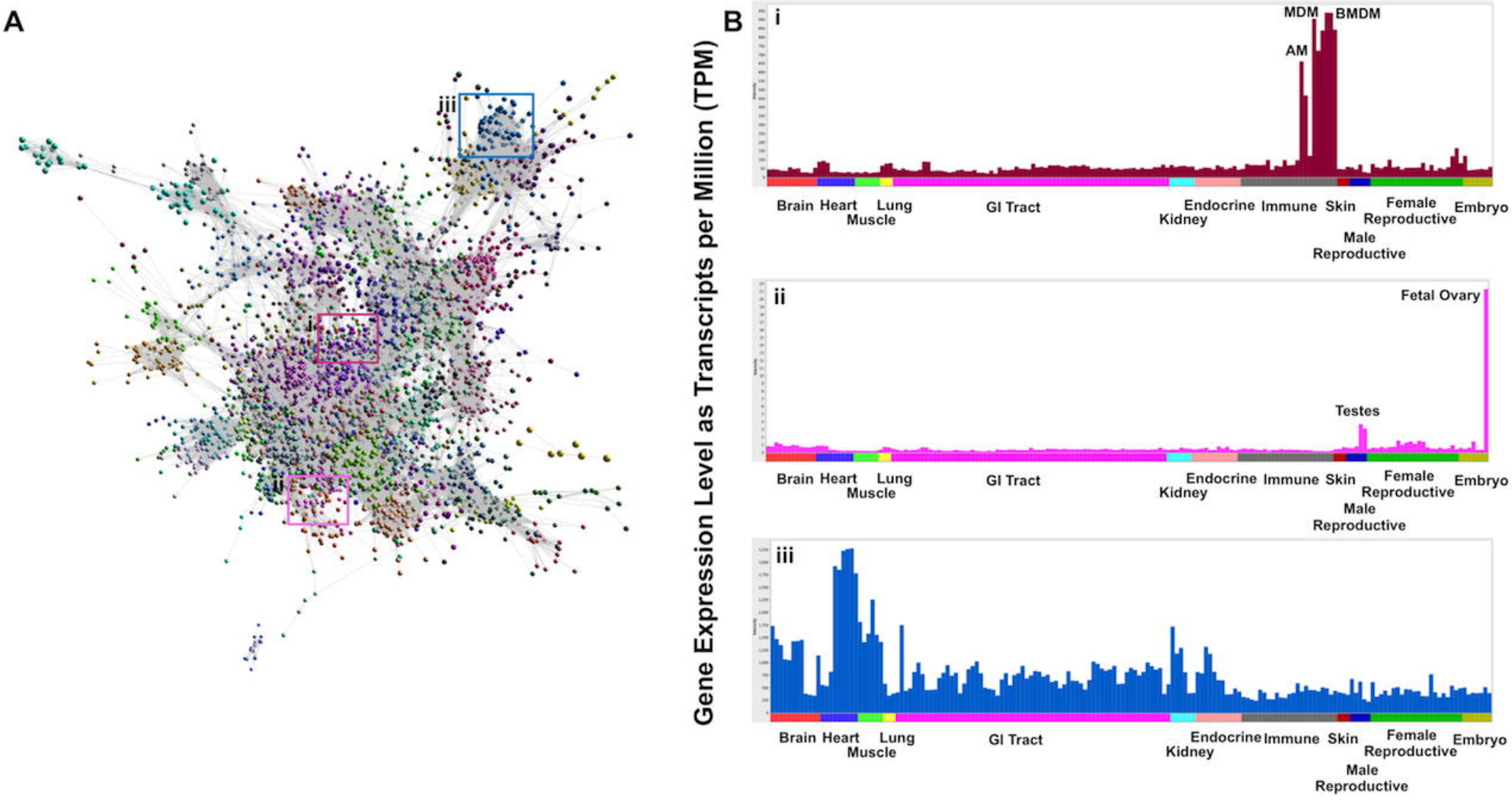
A
iii
i
ii
B
Gene Expression Level as Transcripts per Million (TPM)
i
MDM
BMDM
AM
Brain
Heart
Muscle
Lung
GI Tract
Endocrine
Kidney
Immune
Skin
Female
Reproductive
Male
Reproductive
Embryo
ii
Fetal Ovary
Testes
iii

A

Sire - Texel

Dam – Scottish Blackface

F_1 – Scottish Blackface x Texel

B

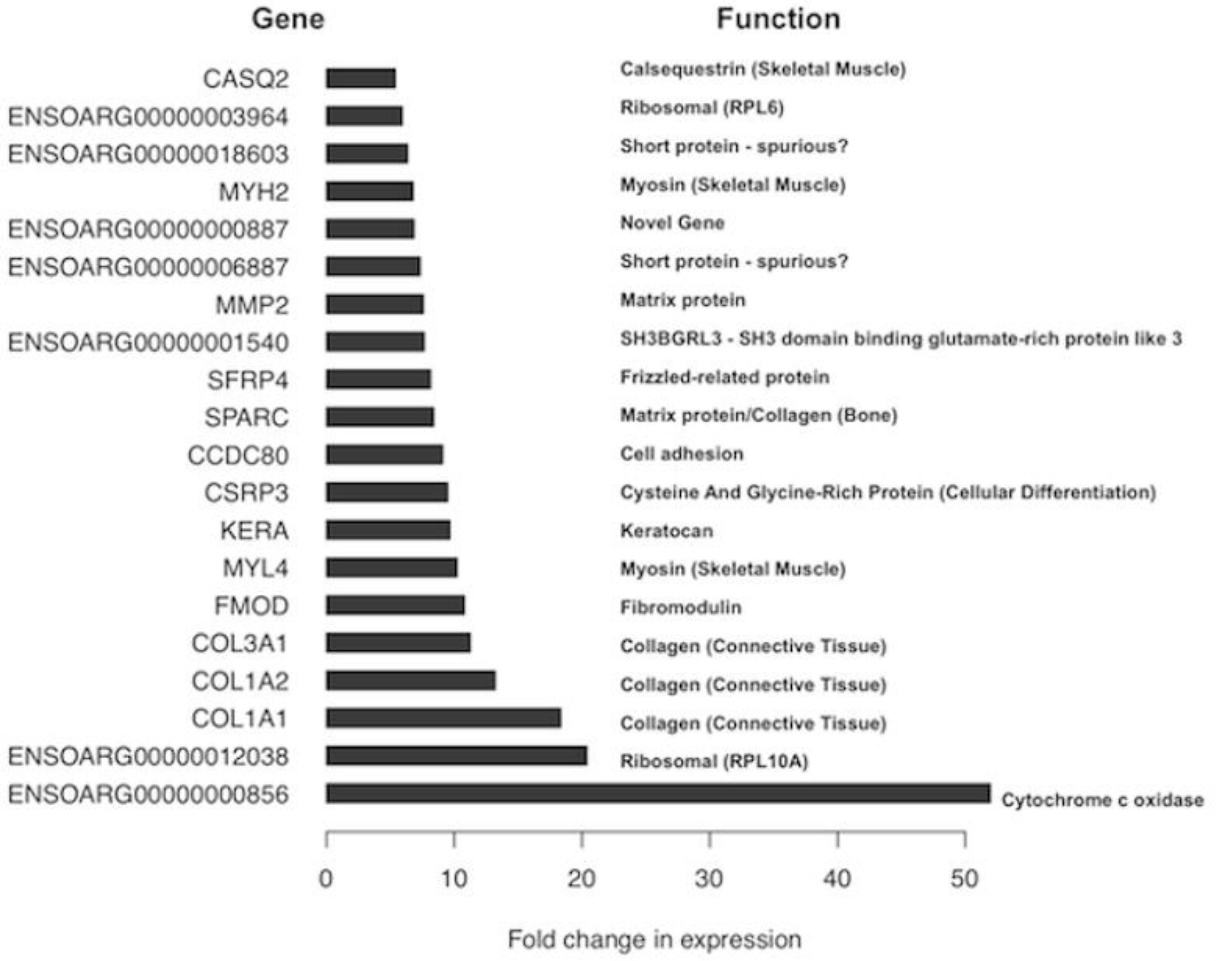

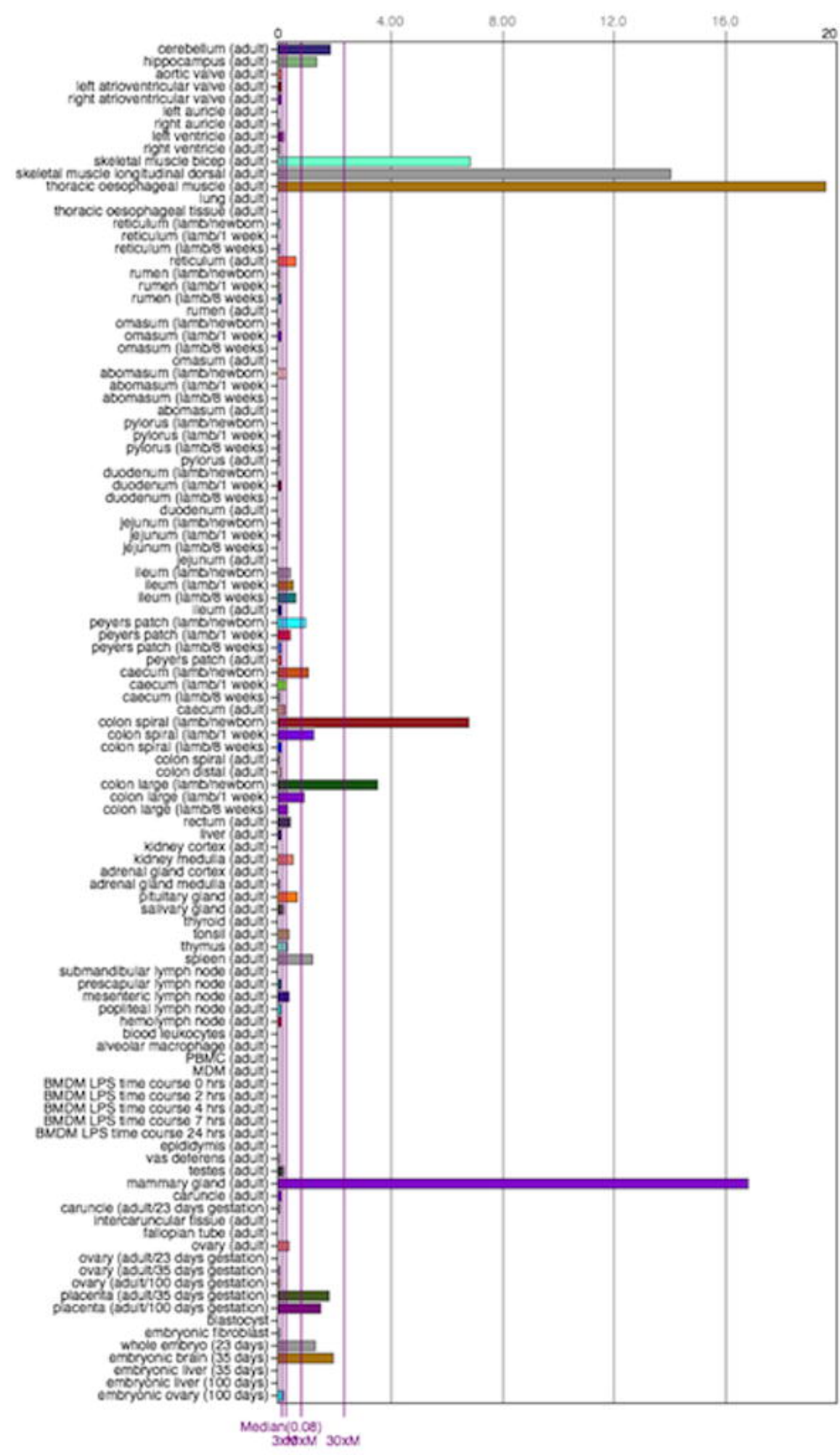
0
4.00
8.00
12.0
16.0
20
cerebellum (adult)
hippocampus (adult)
aortic valve (adult)
left atrioventricular valve (adult)
right atrioventricular valve (adult)
left auricle (adult)
right auricle (adult)
left ventricle (adult)
right ventricle (adult)
skeletal muscle bicep (adult)
skeletal muscle longitudinal dorsal (adult)
thoracic oesophageal muscle (adult)
lung (adult)
thoracic oesophageal tissue (adult)
reticulum (lamb/newborn)
reticulum (lamb/1 week)
reticulum (lamb/8 weeks)
reticulum (adult)
rumen (lamb/newborn)
rumen (lamb/1 week)
rumen (lamb/8 weeks)
rumen (adult)
omasum (lamb/newborn)
omasum (lamb/1 week)
omasum (lamb/8 weeks)
omasum (adult)
abomasum (lamb/newborn)
abomasum (lamb/1 week)
abomasum (lamb/8 weeks)
abomasum (adult)
pylorus (lamb/newborn)
pylorus (lamb/1 week)
pylorus (lamb/8 weeks)
pylorus (adult)
duodenum (lamb/newborn)
duodenum (lamb/1 week)
duodenum (lamb/8 weeks)
duodenum (adult)
jejunum (lamb/newborn)
jejunum (lamb/1 week)
jejunum (lamb/8 weeks)
jejunum (adult)
ileum (lamb/newborn)
ileum (lamb/1 week)
ileum (lamb/8 weeks)
ileum (adult)
peyers patch (lamb/newborn)
peyers patch (lamb/1 week)
peyers patch (lamb/8 weeks)
peyers patch (adult)
caecum (lamb/newborn)
caecum (lamb/1 week)
caecum (lamb/8 weeks)
caecum (adult)
colon spiral (lamb/newborn)
colon spiral (lamb/1 week)
colon spiral (lamb/8 weeks)
colon spiral (adult)
colon distal (adult)
colon large (lamb/newborn)
colon large (lamb/1 week)
colon large (lamb/8 weeks)
rectum (adult)
liver (adult)
kidney cortex (adult)
kidney medulla (adult)
adrenal gland cortex (adult)
adrenal gland medulla (adult)
pituitary gland (adult)
salivary gland (adult)
thyroid (adult)
tonsil (adult)
thymus (adult)
spleen (adult)
submandibular lymph node (adult)
prescapular lymph node (adult)
mesenteric lymph node (adult)
popliteal lymph node (adult)
hemolymph node (adult)
blood leukocytes (adult)
alveolar macrophage (adult)
PBMC (adult)
MDM (adult)
BMDM LPS time course 0 hrs (adult)
BMDM LPS time course 2 hrs (adult)
BMDM LPS time course 4 hrs (adult)
BMDM LPS time course 7 hrs (adult)
BMDM LPS time course 24 hrs (adult)
epididymis (adult)
vas deferens (adult)
testes (adult)
mammary gland (adult)
caruncle (adult)
caruncle (adult/23 days gestation)
intercaruncular tissue (adult)
fallopian tube (adult)
ovary (adult)
ovary (adult/23 days gestation)
ovary (adult/35 days gestation)
ovary (adult/100 days gestation)
placenta (adult/35 days gestation)
placenta (adult/100 days gestation)
blastocyst
embryonic fibroblast
whole embryo (23 days)
embryonic brain (35 days)
embryonic liver (35 days)
embryonic liver (100 days)
embryonic ovary (100 days)
Median(0.08)
3xM
30xM